People's Democratic Republic of Algeria

Ministry of Higher Education and Scientific Research

University of Hamma Lakhdar El-Oued
Faculty of Science and Technology

Department of Electrical Engineering

Dissertation to obtain the Academic Master Degree

Field: Science and Technology

Sector: Telecommunications

Specialty: Telecommunication Systems

Project:

PAPR REDUCTION TECHNIQUES FOR VLC-OFDM SYSTEM

Submitted by:
Slimane MANSOURA

Supervised by:
D. Ridha TOUHAMI

September 2020

Acknowledgment:

First and foremost, my many thanks to Allah for all his blessings. I would also like to express my sincere thanks and gratitude to my family especially my parents for the unconditional support and patience throughout my life.

I am also very grateful to Dr. Ridha TOUHAMI for the knowledge he provided me as well as the support, supervision, guidance and availability to answer my questions during the preparation of this dissertation. Last but not least, I would like to thank the faculty of Technology for giving me the chance to continue my studies.

Abstract:

Visible light communication (VLC) is a new and promising technology from the field of optical wireless communication (OWC) exploiting the visible spectrum for data transmission, that emerged as a solution for radio frequencies (RF) communication systems due to wide available bandwidth, unregulated visible spectrum, and non-existent electromagnetic interference. Alongside, orthogonal frequency division multiplexing (OFDM) is used as a modulation technique for VLC since is capable of transmitting at high data rates and high spectral efficiency as well as reducing the effects of inter-symbol interference (ISI) and inter-carrier interference (ICI). In this dissertation, the aim is to study the OFDM and the adaptation of this modulation for the VLC system to make it use the intensity-modulation/direct-detection (IM/DD) combined with the OFDM signal that modulating the current of LEDs and photodetectors are used for detection, furthermore, we'll view the techniques that may be employed to reduce the PAPR problem which can destroy OFDM structure.

As a summary of the knowledge we got, it will be simulated on MATLAB like an experience of telecommunication channel using Optical-OFDM and SLM technique like a PAPR reduction method.

Keywords:

visible spectrum, electromagnetic interference, high data rates, intensity-modulation, direct-detection, LED, photodetectors.

ملخص:

الاتصالات الضوئية المرئية (VLC) هي تقنية جديدة وواعدة من مجال الاتصالات اللاسلكية الضوئية (OWC) تستغل الطيف المرئي لنقل البيانات ، والتي ظهرت كحل لأنظمة اتصالات الترددات الراديوية (RF) نظرًا لعرض النطاق الترددي المتاح ،كما أن الطيف المرئي مجاني إلى جانب ذلك التداخل الكهرومغناطيسي معدوم. يتم استخدام التجميع التعامدي بتقسيم التردد(OFDM) كتقنية تعديل لـ VLC نظرًا لأنه قادر على الإرسال بمعدلات بيانات عالية وكفاءة طيفية عالية بالإضافة إلى تقليل آثار التداخل بين الرموز (ISI) والتداخل بين الموجات الحاملة .(ICI) الهدف في هذه الرسالة هو دراسة OFDM وتكييف هذا التعديل لنظام VLC لجعله يستخدم تعديل الشدة / الكشف المباشر (IM / DD) جنبًا إلى جنب مع إشارة OFDM التي تعدل تيار الثنائي الباعث للضوء (LED) و يتم استخدام المستشعر الضوئي للكشف الإشارات المرسلة ، علاوة على ذلك ، سنعرض التقنيات التي يمكن استخدامها لتقليل مشكلة PAPR التي يمكن أن تدمر هيكل.OFDM

سيتم محاكاة ملخص المعارف التي حصلنا عليها على MATLAB كتجربة لقناة اتصالات باستخدام تقنية Optical-OFDM و SLM كطريقة تقليل PAPR

الكلمات الرئيسية:

الطيف المرئي ، التداخل الكهرومغناطيسي ، معدلات البيانات العالية ، تعديل الشدة ، الكشف المباشر ، LED ، استخدام المستشعر الضوئي.

Résumé :

La communication par lumière visible (VLC) est une nouvelle technologie prometteuse du domaine de la communication optique sans fil (OWC) exploitant le spectre visible pour la transmission de données, qui a émergé comme une solution pour les systèmes de communication radiofréquences (RF) en raison de la plus grande bande passante disponible, spectre visible libre et interférences électromagnétiques inexistantes. Parallèlement, le multiplexage par répartition orthogonale de la fréquence (OFDM) est utilisé comme technique de modulation pour VLC car il est capable de transmettre à des débits de données élevés et à une efficacité spectrale élevée, ainsi que de réduire les effets des interférences inter-symboles (ISI) et inter-porteuses (ICI). Dans cette thèse, l'objectif est d'étudier l'OFDM et l'adaptation de cette modulation pour le système VLC pour lui faire utiliser la modulation d'intensité / détection directe (IM / DD) combiné avec le signal OFDM qui modulant le courant de la LED et un photo-détecteur est utilisé pour la détection, en outre, nous allons voir les techniques qui peuvent être employées pour réduire le problème PAPR qui peut détruire la structure OFDM.
le résumé des connaissances acquises sera simulé sur MATLAB comme une expérience de canal de télécommunication utilisant la technique Optique-OFDM et SLM comme une méthode de réduction PAPR.

Mots-clés :

spectre visible, interférences électromagnétiques, débits de données élevés, modulation d'intensité, détection directe, LED, photodétecteurs.

Table of Contents:

Chapter 2: Visible Light Communication

Chapter 3: Peak-to-Average Power Ratio

List of figures:

List of Tables:

Abbreviations:

ADC	analog-to-Digital Converter
ADSL	asymmetric Digital Subscriber Line
ACI	adjacent channel interference
ACO-OFDM	asymmetrically clipped optical OFDM
AM	amplitude Modulation
ATM	asynchronous transfer mode
AWGN	additive white Gaussian noise
BERs	bit error rates
BPF	base pass filter
B-PSK	binary Phase-shift keying
C2C	chip-to chip
CCDF	complementary cumulative distribution function
CDF	cumulative distribution Function
CO2	carbon dioxide
CP	cyclic prefix
CS	cyclic suffix
D2D	devise-to-device
DAB	digital audio broadcasting
DAC	digital-to-analog converter
DCO-OFDM	direct current-biased optical
DFT	discrete Fourier transform
DFT	discrete Fourier transformation
DMT	discrete multitone modulation
D-PSK	differential Phase-shift keying
DVB-T	digital video broadcasting terrestrial
EM	electromagnetic
FDD	frequency-division duplexing
FD	frequency division
FDM	frequency division multiplexing
FFT	fast Fourier transform
FM	frequency modulation
FOV	field of view
FSO	Free space optics
HD	high-definition
HS	Hermitian symmetry
ICI	inter-carrier Interference
IDFT	inverse discrete Fourier transform
IFFT	inverse fast Fourier transform
IM/DD	intensity modulation and direct detection
IoT	Internet-of-things
IR	infrared
ISI	Inter-symbol Interference
LE	light-emitting diode
LDs	laser diodes
LoS	line-of-sight
LPF	low pass filter
LTE	long-term evolution
M2M	machine-to-machine
MB-OFDM	multiband OFDM
MIMO	multiple-input and multiple-output

mm-Wave	millimetre wave
OCC	optical camera communications
OFDM	orthogonal frequency division multiplexing
O-OFDM	optical-OFDM transmission system
OWC	optical wireless communication
PAPR	peak-to-average Ratio
PA	pilot-assisted
PDs	photo-diodes
PM	phase Modulation
PN	pseudorandom noise
PSD	power spectral density
PTS	partial transmit sequences
QAM	quadrature amplitude modulation
QPSK	quadrature phase-shift keying
RC	raised cosine
RF	radio frequency
rms	root mean squared
RSC	recursive systematic convolutional
SCM	single carrier modulation
SE	spectral efficiency
SI index	side information index
SISO	soft input soft output
SLM	selected-mapping
SQNR	signal-to-quantization noise ratio
STO	shift time offset
TD	time division
THz	terahertz
TR	tone-reservation
TTI	transmission Time Interval
TV	television
UWB	ultra wide-band
UV	ultraviolet
UMTS	Universal Mobile Telecommunications Service
V2X	vehicle-to-infrastructure
V2V	vehicle-to-vehicle
VCs	virtual carriers
VDSL	very high speed digital subscriber line systems
VLC	visible light communication
VL	visible light
WBAN	wireless body area network
Wi-Fi	wireless fidelity
WIMAX	worldwide interoperability for microwave access
WLANs	wireless local area networks
WPAN	wireless personal area network
ZP	zero padding

INTRODUCTION

Due to the increasing requirement for high data-rates in modern communication systems, Orthogonal Frequency Division Multiplexing (OFDM) has been intensively studied over the last two decades. OFDM as a modulation mechanism provides a high data-rate with robustness against a multipath fading channel. Moreover, the OFDM technique is widely used in wired and wireless communications because of its poplar advantages for reducing interference and multipath issues compared with conventional single-carrier modulation (SCM) techniques. The unique feature of the OFDM technique is the use of orthogonality between the individual subcarriers. Furthermore, the importance of OFDM is that it has the best spectral efficiency to Radio Frequency (RF) interference.

OFDM has been also implemented in Visible light communication (VLC) system to complete conventional wireless communication due the RF spectrum resource is becoming saturated and the existing RF-based wireless communication system will not meet the demands for data traffic in the future. For that matter a significant research effort has been directed towards the development of VLC systems due their numerous advantages, such as the use of visible light for communication as well as illumination, unlicensed spectrum, and the potentially high data-rates that can be achieved besides the VLC system can serve different areas with wireless signals that are hard to reach with conventional RF systems.

However, there are several challenges facing the implementation of OFDM in the VLC system (i.e. Optical-OFDM) to achieve high data rates (multi gigabits per second). These challenges include the inter-channel interference (ICI), inter-symbol interference (ISI) due to multipath propagation, and high PAPR which can affect the Optical-OFDM signals as much as the RF-OFDM signals. High PAPR has been cited as one of the major drawbacks of the OFDM modulation format, the problem resides in the optical source at the transmitter's end, where the optical source gain will saturate at the high input power.

This dissertation focuses on the first chapter about study the channel characterizations and propagations features, OFDM system execution methods, the advantage, disadvantages, and applications. As we will expose in the second chapter, the visible light communication (VLC) system, its principals, implementation, application, advantage and disadvantage. Then we'll see how to optimize the OFDM performance for the indoor optical wireless systems (VLC) witch use free-space and also employ intensity modulation with direct detection. The third chapter, we'll talk about the techniques used to reduce high PAPR. Finally, we will summarize all the knowledge gotten in the final conclusion.

Based on the information gained, we'll simulate on MATLAB a telecommunication channel using Optical-OFDM and SLM technique like a PAPR reduction method.

CHAPTER I:

ORTHOGONAL FREQUENCY DIVISION MULTIPLEXING

1.1. Introduction:

High data-rate is desirable in many recent wireless multimedia applications. Traditional single carrier modulation techniques can achieve only limited data rates due to the restrictions imposed by the multipath effect of wireless channel and the receiver complexity. Orthogonal Frequency Division Multiplexing (OFDM) is a prominent candidate to fulfill the requirements of current and next generation wireless communication systems. However, Peak-to-Average Ratio (PAPR), Inter-symbol Interference (ISI) and Inter-carrier Interference (ICI) are major challenges in implementing an OFDM system. In this chapter we represent the channel characterizations and the signal propagation analysis in order to figure-out how the transmission medium can effect on the signal and how multipath occurs. Then, we'll expose the OFDM system with the signal generation technology using IFFT/FFT blocs and the solutions of some constraints facing the OFDM system. Finally, we'll talk about the advantage, disadvantage and the applications of the OFDM system in the different telecommunications categories.

1.2. Channel characterizations:

The wireless mobile channel's time-varying nature makes the characterization of the channel and its analysis a significant question. The time-varying existence of the channel might be observed in several different forms in a mobile wireless situation, e.g. a relative motion between the transmitter and the receiver, time variation in the medium structure, etc. All these situations randomize the characteristics of the channel and provide no easy analysis of the transmitted signals. Generally, as an information signal propagates through the channel, as the distance between the transmitter and receiver increases, the strength of this signal decreases. The received signal strength depends on the Channel characteristics and the distance between the transmitter and the receiver. The channel can be modelled in a broad sense in two distinct categories, the large-scale propagation model and the small-scale propagation model. [**Ibn04**]

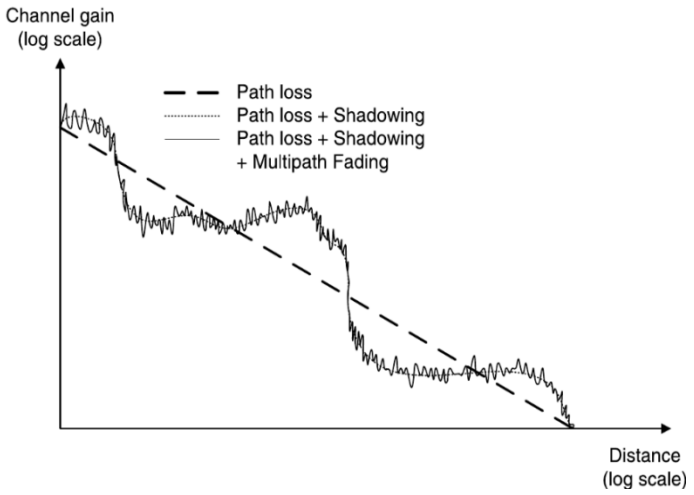

Figure 1-1: Small Scale Propagation Fading VS Large Scale Propagation Fading.

1.2.1. Large-Scale Propagation Models:

It's defining the strength of the received signal over large transmitter-receiver separation distances of several hundred or thousands of meters, there are usually categorized into two classifications: deterministic and stochastic. In describing a time-varying channel, both deterministic and stochastic models are useful, but they support different aspects: the stochastic model is best suited for explaining global actions, while the deterministic one is more useful for analysing the propagation through a particular channel realization. [**Ibn04**]

1.2.1.1. Deterministic Approach:

1.2.1.1.1. Free-Space Propagation Model:

In this model, the received signal power declines as a function of the distance between the transmitter and the receiver while a clear line of sight separate them. In this case, the free-space signal power $\boldsymbol{P_t(d)}$, received by the antenna at a distance $\boldsymbol{d}$ (meters) from the transmitter, is given by

$$\boldsymbol{P_r(t) = \frac{P_t G_t G_r \lambda^2}{(4\pi)^2 d^2 L} \quad d \geq d_0 (\neq 0) \geq d_f} \tag{1.1}$$

where $\boldsymbol{P_t}$, represents the transmitted signal power, $\boldsymbol{G_t}$, and $\boldsymbol{G_r}$, are the transmitter and receiver antenna gains respectively, $\boldsymbol{L(\geq 1)}$ is the system loss factor, independent of signal propagation, $\boldsymbol{\lambda}$ (meters) is the wavelength, $\boldsymbol{d_f}$ is the far-field distance (also known as Fraunhofer distance), and $\boldsymbol{d_0}$ is the received-power reference distance. The far-field distance $\boldsymbol{d_f}$, is given by

$$\boldsymbol{d_f = \frac{2D^2}{\lambda} d_f \quad \gg D} \tag{1.2}$$

where $\boldsymbol{D}$ is the largest physical linear dimension of the antenna. Using Equation (1.1), the free-space received power at a distance $\boldsymbol{d} > \boldsymbol{d_0}$ can be written as [**Ibn04**]

$$\boldsymbol{P_r(d) = P_r(d_0)\left(\frac{d}{d_0}\right)^{-2}} \tag{1.3}$$

1.2.1.1.2. Log-Distance Path Loss Model:

This model shows that the average path loss[1] increases logarithmically with distance between the transmitter and the receiver, which is given by

[1] Path loss, expressed in dB, is defined as the difference between the effective transmitted signal power and the received signal power.

$$\boldsymbol{Pl_{avg}(dB) = Pl_{avg}(d_0) + 10\,n\,log\left(\frac{d}{d_0}\right)} \tag{1.4}$$

where $\boldsymbol{n}$ is the path loss exponent that indicates the rate at which the path loss for the transmitted signal increase with the distance. The value of $\boldsymbol{n}$ depending on specific propagation environment (e.g. see the Table: 1.1) [**Ibn04**]

environment	Path loss exponent (n)
Free space	2
Urban area cellular radio	2.7-3.5
Shadowed urban cellular radio	3-5
In building line-of sight	1.6-1.8
Obstructed in building	4-6
Obstructed in factories	2-3

Table 1.1: Path Loss Exponent for Different Communication Environment

1.2.1.2. Stochastic Approach:

1.2.1.2.1. Lognormal Shadowing Model:

Lognormal shadowing model is the phenomenon that describes the random shadowing effects that occur over a large number of sampling sites that have the same transmitter and receiver separation with various levels of clutter on the propagation path. The corresponding path loss model states that the path loss $\boldsymbol{Pl(d)}$ at a particular location is lognormally (normal in dB) distributed about the mean distance-dependent value. The analytical expression of this model is given by

$$\begin{aligned} \boldsymbol{Pl(d)} &= \boldsymbol{Pl_{avg}(d) + X_\sigma} \\ &= \boldsymbol{Pl_{avg}(d_0) + 10\,n\,log\left(\frac{d}{d_0}\right) + X_\sigma} \end{aligned} \tag{1.5}$$

where $\boldsymbol{X_\sigma}$ (dB) is a zero-mean Gaussian distributed random variable with a variance of $\boldsymbol{\sigma^2}$ dB. In general, the values of $\boldsymbol{n}$ (defined earlier) and $\boldsymbol{\sigma^2}$ are computed from measured data (e.g., see Table 3.6 in Rappaport [**Rap96**]), using linear regression in such a way that the contrast between the estimated and measured path losses is minimized.

Other than the general large-scale propagation models described above, there are some specific models based on the outdoor and indoor environments separately. These channels models are based on the profile of the particular area. Examples of some outdoor propagation models include the Durkin's model [**Dad75**] and Longley-Rice model [**Lon68**]. Examples of some indoor models are the attenuation factor model [**Sei92**] and the Erricson multiple break-point model [**Ake88**]. In addition to these models, Ray tracing and site-specific modeling techniques are also used for both outdoor and indoor environments. [**Ibn04**]

1.2.2. Small-Scale Propagation Models:

These models show the strength of the received radio signal over a limited period of time or travel distance of typically 5 $\boldsymbol{\lambda}$ to 40 $\boldsymbol{\lambda}$.The instantaneous received signal fluctuates very quickly in this scenario and can give rise to fading, which is called small-scale fading. We will address various small-scale propagation models in this section by providing all the necessary parameters needed
[**Ibn04**]

1.2.2.1. Parameters of Mobile Multipath Channel:

Many significant parameters characterize a multipath channel. The time-dispersive nature of the channel in a local area is defined by the delay spread and coherence bandwidth parameters. In a small-scale area, on the other hand, Doppler spread and coherence bandwidth define the time-varying nature of the channel. Including these key parameters, the channel parameters will be briefly addressed here, offering a detailed overview of a mobile multipath channel. [**Ibn04**]

1.2.2.1.1. Fading:

The interference between two or more attenuated versions of the transmitted signal arriving at the receiver is the result of fading, also known as small-scale fading, in such a way that these signals are added destructively. These multiple transmitted signal versions are the result of multiple paths in the channel, or rapid dynamic shifts in the channel. In this situation, the mobile speed and signal bandwidth of the transmission also play a critical role. [**Ibn04**]

1.2.2.1.2. Doppler Shift:

The apparent change in frequency of the transmitted signal due to the relative motion of the mobile is known as the Doppler shift, which is given by

$$f_{ds} = \frac{v}{\lambda} cos\theta \tag{1.6}$$

where $\boldsymbol{v}$ is the velocity of the mobile, $\boldsymbol{\lambda}$ is the signal wavelength, and $\boldsymbol{\theta}$ is the spatial angle between the direction of motion of the mobile and the direction of arrival of the wave.[**Ibn04**]

1.2.2.1.3. Excess Delay:

This is the relative delay of the $\boldsymbol{i}$th multipath signal component, compared to the first arriving component and is given by $\boldsymbol{\tau_i}$. [**Ibn04**]

1.2.2.1.4. Power Delay Profile $\Phi_c(\tau)$:

It's the channel's average output signal power as a function of the excess time delay $\boldsymbol{\tau}$. Practically, $\Phi_c(\boldsymbol{\tau})$ is measured by transmitting very narrow pulses, or equivalently a wide band signal, and cross-correlating the received signal with a delayed version of itself. Power delay profile can sometimes be referred to as *multipath intensity profile* and *delay power spectrum*. It gets the latter name because of its frequency domain component, which gives the

power spectrum density. The mean excess delay, root mean squared (rms) delay spread, and excess delay spread (***X*** dB) are multipath channel parameters that can be determined from a power delay profile. The mean excess delay ($\boldsymbol{\tau_{mean}}$) is the first moment of the power delay profile, the rms delay spread ($\boldsymbol{\sigma_\tau}$) is the square root of the second central moment of the power delay profile, and the maximum excess delay (***X*** dB) of the power delay profile is defined as the time delay during which multipath energy falls to ***X*** dB below the maximum value. $\boldsymbol{\tau_{mean}}$ and $\boldsymbol{\sigma_\tau}$ are expressed as [**Ibn04**]

$$\boldsymbol{\tau_{mean}} = \frac{\sum_i \boldsymbol{P(\tau_i)\tau_i}}{\sum_i \boldsymbol{P(\tau_i)}} \tag{1.7}$$

$$\boldsymbol{\sigma_\tau} = \sqrt{\boldsymbol{mean}[(\tau)^2] - (\boldsymbol{\tau_{mean}})^2} \tag{1.8}$$

where

$$\boldsymbol{mean}[(\tau)^2] = \frac{\sum_i \boldsymbol{P(\tau_i)\tau_i}^2}{\sum_i \boldsymbol{P(\tau_i)}} \tag{1.9}$$

Tab	Relative delay (*ns*)	Average power (*dB*)
1	0	0.0
2	110	-9.7
3	190	-19.2
4	410	-22.8

Table 1.2: Power Delay Profile (example (ITU-R Pedestrian A Model)

1.2.2.1.5. Delay Spread (T_m):

Delay spread, also known as *multipath spread*, of the channel is the range of values of excess delay $\boldsymbol{\tau}$ over which $\Phi_c(\boldsymbol{\tau})$is essentially nonzero. [**Ibn04**]

1.2.2.1.6. Coherence Bandwidth (BW_{coh}):

The frequency band in which all of the transmitted signal's spectral components pass through a channel with equivalent gain and linear phase is identified as coherence bandwidth of that channel. Over this bandwidth the channel remains invariant. $\boldsymbol{BW_{coh}}$ can be expressed in terms of rms delay spread, through there is no exact relationship between these two parameters. According to Lee [**Lee89**] with the frequency correlation of approximately 90%, $\boldsymbol{BW_{coh}}$ can be shown as

$$\boldsymbol{BW_{coh}} \approx \frac{\mathbf{1}}{\mathbf{50}\boldsymbol{\sigma_\tau}} \tag{1.10}$$

1.2.2.1.7. Doppler Spread (Ba):

Spreading of the frequency spectrum of the transmitted signal resulting from the rate of change of the mobile radio channel is known as Doppler spread. With the transmitted signal frequency f_c, the resultant Doppler spectrum has the components in the range between $(f_c - f_{d,max})$ and $(f_c + f_{d,max})$), $f_{d,max}$ being the maximum Doppler frequency shift. [Ibn04]

1.2.2.1.8. Coherence Time (T_{coh}):

The period of time during which the response of the channel impulse remains invariant is known as coherence time of the channel. T_{coh} is inversely proportional to the Doppler spread, and with the maximum Doppler frequency shift, $f_{d,max}$ it is given by [Ibn04]

$$T_{coh} \approx \frac{1}{f_{d,max}} \tag{1.11}$$

1.2.2.2. Types of Small-Scale Fading:

Small-scale fading, based on the time delay spread and Doppler spread, is mainly divided into two categories. The time delay spread-dependent class is classified into two groups, flat fading and frequency-selective fading, while fast and slow fading is categorized as the Doppler spread-dependent class. It is important to remember that the relationship between the time rate of change of the channel and the transmitted signal is done by fast and slow fading, and not with propagation path loss models.[Ibn04]

1.2.2.2.1. Flat Fading:

If the channel has a constant gain and linear phase response over a bandwidth that is greater than the bandwidth of the transmitted signal, the received signal in a mobile radio setting experiences flat fading. The primary features of a flat fading channel follow:

- Symbol period of the transmitted signal is greater than the delay spread of the channel. As a rule of thumb it should be at least 10 times greater.
- Bandwidth of the channel is greater than the bandwidth of the transmitted signal. Since the bandwidth of the transmitted signal is narrower than the channel bandwidth, the flat fading channels are also known as *narrowband channels*.
- Typical flat fading channels result in deep fades, and this requires 20 to 30 dB more transmitter power to achieve low bit error rates (BERs) during times of deep fades, compared to systems operating over nonfading channels. [Ibn04]

1.2.2.2.2. Frequency-Selective Fading:

In a mobile radio system, the received signal experiences frequency-selective fading if the channel has a steady gain and linear phase response over a bandwidth that is smaller than the transmitted signal bandwidth. The main features of a frequency-selective fading channel are follow:

- Symbol period of the transmitted signal is smaller than the delay spread of the channel. As a rule of thumb it should be at least 10 times smaller.
- Bandwidth of the channel is smaller than the bandwidth of the transmitted signal. Since the bandwidth of the transmitted signal is wider than the channel bandwidth, the frequency-selective fading channels are also known as *wideband channels*.
- Frequency-selective channel results in inter-symbol interference (ISI) for the received signal.
- This type of fading channels is difficult to model compared to the flat fading channels since each multipath signal needs to be modeled individually and the channel has to be considered as a linear filter. [**Ibn04**]

1.2.2.2.3. Fast Fading:

In a mobile radio system, the received signal experiences rapid fading as a result of rapidly changing channel impulse response within the period of the symbol. The primary features of a fast fading channel are follow:

- Coherence time of the channel is smaller than the symbol period of the transmitted signal. Thus this is also called *time-selective fading*.
- Doppler spread is greater than the transmitted signal bandwidth.
- Channel varies faster than the baseband signal variations.
- In *fast-flat fading* channels the amplitude of the received signal varies faster than the rate of change of the transmitted baseband signal.
- In *fast-frequency-selective* channels the amplitudes, phases, and time delays of the multipath components vary faster than the rate of change of the transmitted signal. [**Ibn04**]

1.2.2.2.4. Slow Fading:

In a mobile radio system, the received signal experiences slow fading as a result of slowly changing channel impulse response throughout the length of the symbol. The primary features of a slow fading channel follow:

- Coherence time of the channel is greater than the symbol period of the transmitted signal. In this case, the channel can be assumed to be static over one or several symbol durations.
- Doppler spread is smaller than the transmitted signal bandwidth.
- Channel varies slower than the baseband signal variations.[**Ibn04**]

1.3. Modulation Technique:

Modulation is a carrier signal that varies in accordance with the message signal. Modulation technique is used to change the signal characteristics. Basically, the modulation is of following two types:

- Analog Modulation
- Digital Modulation

1.3.2. Analog Modulation:

Modulation is a process in which a modulator changes some attribute of a higher frequency carrier signal proportional to a lower frequency message signal. If the carrier is represented by the equation:

$$\boldsymbol{A_c\, cos(2\pi f_c t + \emptyset)} \tag{1.12}$$

While $\boldsymbol{A_c}$: carrier amplitude, $\boldsymbol{f_c}$: carrier frequency, $\emptyset$: carrier phase

a change in the message signal will produce a corresponding change in either the amplitude (Amplitude Modulation AM), frequency (Frequency Modulation FM), or phase (Phase Modulation PM) of the carrier. A transmitter can then send this carrier signal through the communication medium more efficiently than the message signal alone.

Since, Analog modulation includes AM, FM and PM is more sensitive to noise. If noise enters into a system, it persists and gets carried up to the end receiver. So, this drawback can be overcome by the digital modulation technique.

1.3.3. Digital Modulation:

For a better quality and efficient communication, digital modulation technique is employed. The main advantages of the digital modulation over analog modulation include available bandwidth, high noise immunity and permissible power. In digital modulation, a message signal is converted from analog to digital message, and then modulated by using a carrier wave. Similar to the analog, in this system, the type of the digital modulation is decided by the variation of the carrier wave parameters like amplitude, phase and frequency. The most important digital modulation techniques are based on keying such as Amplitude Shift Keying, Frequency Shift Keying, Phase Shift Keying, Differential Phase Shift Keying, Quadrature Phase Shift Keying, Minimum Shift Keying, Gaussian Minimum Shift Keying, Frequency Division Multiplexing and Orthogonal Frequency Division Multiplexing, etc.,

In an Amplitude shift keying, the amplitude of the carrier wave changes based on the message signal or on the base-band signal, which is in digital format. It is sensitive to noise and used for low-band requirements. While, in frequency shift keying, the frequency of the carrier wave is varied for each symbol in the digital data. It needs larger bandwidths. Similarly, the phase shift keying changes the phase of the carrier for each symbol and it is less sensitive to noise.

The need for high data rate transmission to meet the demands of existing and emerging data intensive applications and services is one of the key elements driving the research to progress modulations techniques.

1.4. Orthogonal Frequency Division Multiplexing:

OFDM has gained a significant presence in the wireless market place. The combination of high data capacity, high spectral efficiency, and its resilience to interference as a result of multi-path effects means that it is ideal for the high data applications that have become a major factor in today's communication scene.

OFDM is a special case of Frequency division multiplexing (FDM) scheme in which numerous closely spaced orthogonal subcarriers carriers are used for data transmission. Each subcarrier is modulated with a conventional digital modulation scheme (such as QPSK, 16QAM, etc.) at low symbol rate. However, the combination of many subcarriers enables data rates higher than the conventional single-carrier modulation schemes within equivalent bandwidths.

1.4.1. Frequency division Multiplexing:

This technique concern to modulating several low bandwidth signals by different subcarrier frequencies transmitted simultaneously, rather than transmit a high-rate stream of data with a single subcarrier. To avoid interference, the spectra of the modulated band-pass signals must be kept separate by guard bard of unused frequencies. FDM used in the telephone system to multiplex many telephone conversation onto one high capacity line, as well as to carry many digital signals on a single cable in broadband computer networks.

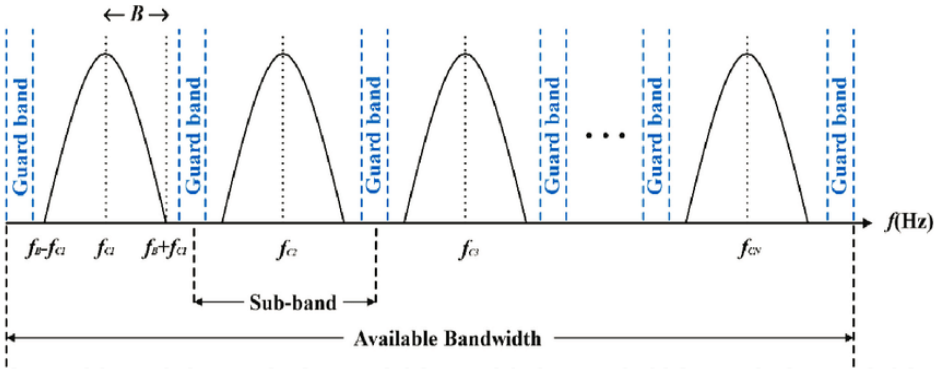

Figure 1-2: FDM Spectra

1.4.2. OFDM Signal Generation Technology:

OFDM is a method of encoding digital signal data on multiple subcarrier frequency and it takes several low data rate frequency channels and then combined them into one high data rate frequency channel. In OFDM data are modulated to time signal and can be generated using Q-PSK, D-PSK, B-PSK etc. Symbols are divided into different frames so that data can be modulated frame by frame during modulation. Figure 1-3 represents an OFDM transmitting a receiving system.

One requirement of the OFDM transmitting and receiving systems is that they must be linear. If any non-linearity appears then it will cause interference between the carriers as a result of inter-modulation distortion. This will introduce unwanted signals that would cause interference and impair the orthogonally of the transmission.

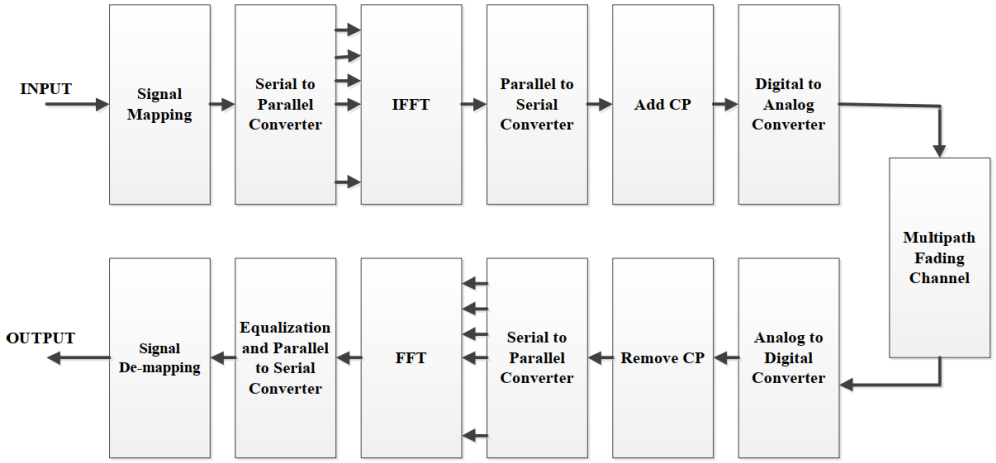

Figure 1-3: OFDM Block Diagram

1.4.2.1. Coding Interleaving and Mapping:

Interleaving and coding are the first blocks inside the transmitter. Both OFDM systems use some form of error correction or detection, since some of the parallel data streams can experience deep fading if there is frequency selective fading in the channel. The coding is usually preceded by interleaving because the frequencies that are experiencing fading may affect a number of adjacent OFDM subcarriers. The data is mapped into complex numbers after coding, representing the QAM constellation that is used for transmission. Usually, constellation sizes from 4 QAM to 256 QAM are used. Although phase shift keying (PSK) is OFDM compliant, it is rarely used.

Unlike PSK in single carrier systems, does not have a constant signal envelope and, for large constellations, has smaller distance between constellation points and so is more susceptible to noise. The sequence of complex numbers output from the constellation mapping are then serial-to-parallel (S/P) converted to form a vector suitable for input to the IFFT. [**Fab10**]

1.4.2.2. FFT and IFFT:

The main component in the transmitter is the Fast Fourier Transform (FFT) block, and in the receiver is the Inverse Fast Fourier Transform (IFFT) block, and these are the functions that distinguish OFDM from single carrier systems.

The input to the IFFT is the complex vector $\boldsymbol{X} = [\boldsymbol{X_0} + \boldsymbol{X_1} + \boldsymbol{X_2} + \cdots + \boldsymbol{X_{N-1}}]^{\boldsymbol{T}}$ the vector has length N, where N is the size of the IFFT. Each of the elements of $\boldsymbol{X}$ represents the data to be carried on the corresponding subcarrier. Usually QAM modulation is used in OFDM, so each of the elements of a complex number representing a particular QAM constellation point. The output of the IFFT is the complex vector $\boldsymbol{x} = [\boldsymbol{x_0} + \boldsymbol{x_1} + \boldsymbol{x_2} + \cdots + \boldsymbol{x_{N-1}}]^{\boldsymbol{T}}$

$$x_m = \frac{1}{\sqrt{N}} \sum_{k=0}^{N-1} X_k \exp\left(\frac{j2\pi km}{N}\right) \qquad \text{for } 0 \le m \le N-1 \tag{1.12}$$

The significant advantage of this type of the IFFT / FFT transform pair is that the discrete signals at the input and output of the transform have the same total energy and same average power for each symbol. The analysis of several OFDM functions is thus simplified. Although the X components take just a few discrete values, the probability distribution of x is not apparent.

In fact for $\boldsymbol{N \geq 64}$ the real and imaginary components of an OFDM time domain signal are approximately Gaussian. For wireless OFDM systems which have already been standardized, values of N ranging from 64 in wireless LAN systems to 8096 in digital television systems have been used.

At the receiver the FFT performs a forward transform on the received sampled data for each symbol

$$Y_k = \frac{1}{\sqrt{N}} \sum_{m=0}^{N-1} y_m \exp\left(\frac{-j2\pi km}{N}\right) \qquad \text{for } 0 \leq k \leq N-1 \tag{1.13}$$

where $\boldsymbol{y = [y_0 + y_1 + y_2 + \cdots + y_{N-1}]^T}$ is the vector representing the sampled time domain signal at the input to the receiver FFT, and $\boldsymbol{Y = [Y_0 + Y_1 + Y_2 + \cdots + Y_{N-1}]^T}$ is the discrete frequency domain vector at the FFT output.

First consider what would happen if there were no noise or distortion in the channel or the transmitter and receiver front ends, then because the FFT and IFFT are transform pairs, thus $\boldsymbol{X = Y}$.

If additive white Gaussian noise (AWGN) is added to the signal, but the signal is not distorted then

$$\boldsymbol{y_m = x_m + w_m} \tag{1.14}$$

Where w_m is a sample of white Gaussian noise substituting (1.4) in (1.5) and rearranging gives:

$$Y_k = \frac{1}{\sqrt{N}} \sum_{m=0}^{N-1} y_m \exp\left(\frac{-j2\pi km}{N}\right) = X_k + W_k \tag{1.15}$$

where

$$W_k = \frac{1}{\sqrt{N}} \sum_{m=0}^{N-1} y_m \exp\left(\frac{-j2\pi km}{N}\right) \qquad for\ 0 \leq k \leq N-1 \tag{1.15}$$

W_K is the noise component of the K_{th} output of the receiver FFT. Because each value of W_K is the summation of independent white Gaussian noise samples w_m it is an independent white Gaussian noise process too. [**Fab10**]

The following Figure 1.4 illustrates inter-relationship between the frequency and time domains. In the frequency domain, multiple adjacent tones or subcarriers are each independently modulated with complex data. An IFFT transform is performed on the frequency-domain subcarriers to produce the OFDM symbol in the time-domain. Then in the time domain, guard intervals are inserted between each of the symbols. Multiple symbols can be concatenated to create the final OFDM burst signal. At the receiver an FFT is performed on the OFDM symbols to recover the original data bits.

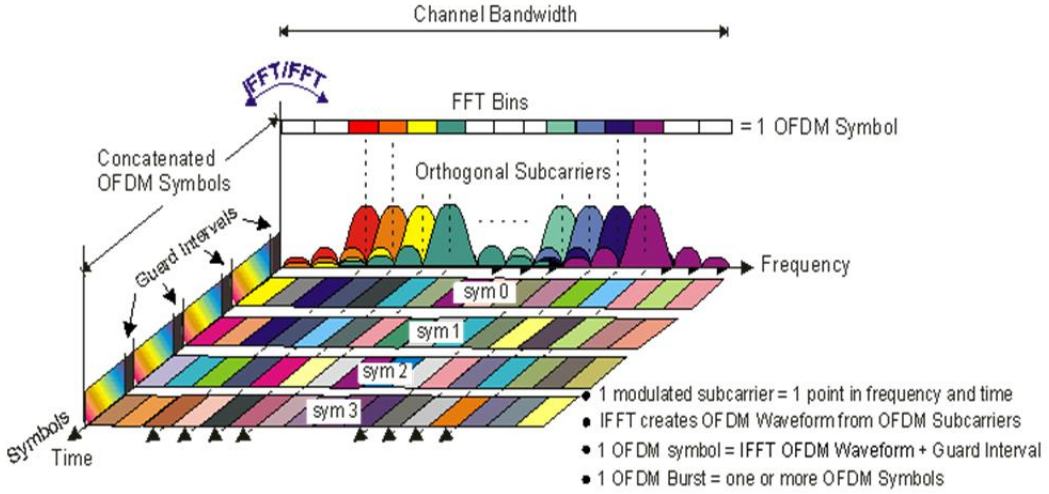

Figure 1-4: Frequency-Time Representative of an OFDM signal

1.4.2.3. The Importance of Orthogonally:

Each transmitted subcarrier results in a spectrum of sinc function with side lobes that generate overlapping spectra between subcarriers- in the frequency domain-, see' OFDM Signal Frequency Spectra' Figure 1.5. This results in subcarrier interference except at orthogonally spaced frequencies there the individual peaks of subcarriers all line up with the nulls of the other subcarriers. The overlap spectral energy doesn't interfere with the ability of the system to restore the original signal. To recover the original set of bits sent, the receiver multiplies (i.e. correlates) the incoming signal with the known set of sinusoids.

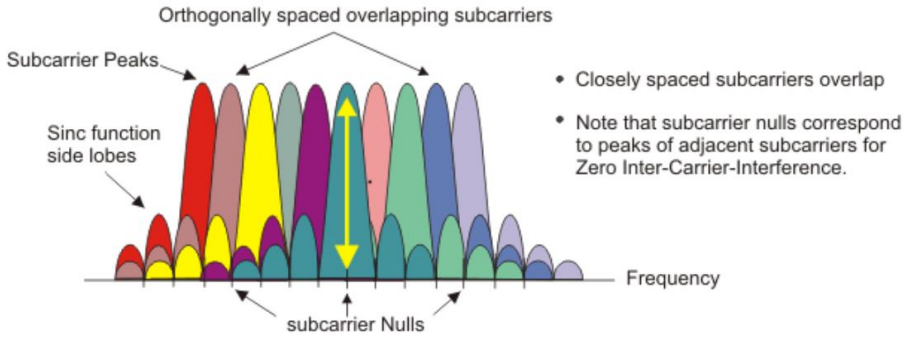

Figure 1-5: OFDM Signal frequency spectra

The use of orthogonal subcarriers makes it possible to improve the spectral efficiency that means more subcarriers per bandwidth. Orthogonality eliminates interference between overlapping carriers in a perfect OFDM signal. In OFDM systems, only when there is a loss

of orthogonality can the subcarriers interfere with each other. For example, frequency error causes the frequencies of the subcarrier to shift, so that the spectral nulls are no longer aligned that resulting in inter-subcarrier-interference. [**Key20**]

1.4.2.4. OFDM Guard Interval:

1.4.2.4.1. Effect of Multipath Channel on OFDM Symbols:

In order to understand an ISI effect of the multipath channel, we consider the illustrative examples for the discrete-time channel in Figure 1-6, where two impulse responses with different lengths are shown along with their frequency responses. Figure 1-7 illustrates an ISI effect of the multipath channel over two consecutive OFDM symbols. Let $\boldsymbol{T_{sub}}$ denote the duration of the effective OFDM symbol without guard interval. Since $\boldsymbol{W = 1/T_s}$ and thus, $\boldsymbol{\Delta f = W/N}$ and $\boldsymbol{T_{sub} = NT_s}$. By extending the symbol, the effect of the multipath fading channel is greatly reduced on the OFDM symbol. However, its effect still remains as a harmful factor that may break the orthogonality among the subcarriers in the OFDM scheme. [**Yon10**]

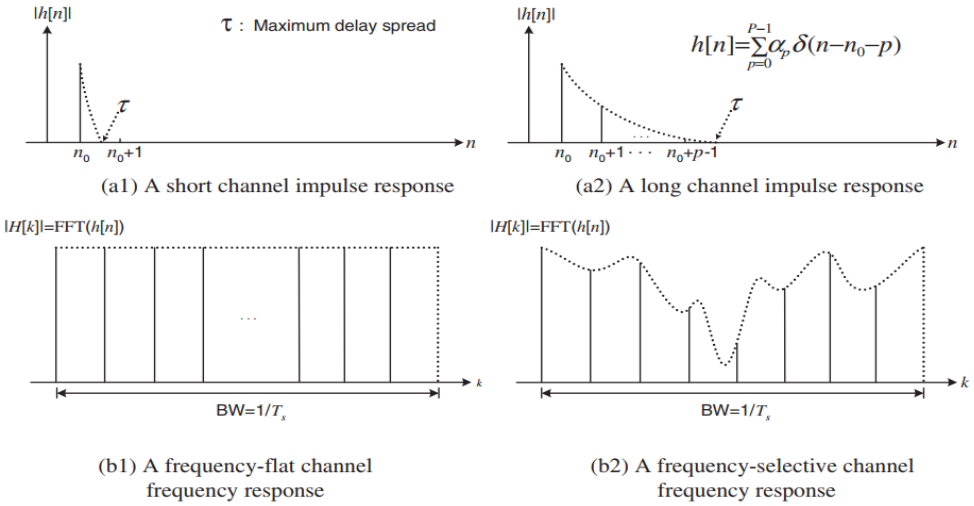

Figure 1-6: Impulse/frequency responses of a discrete-time channel

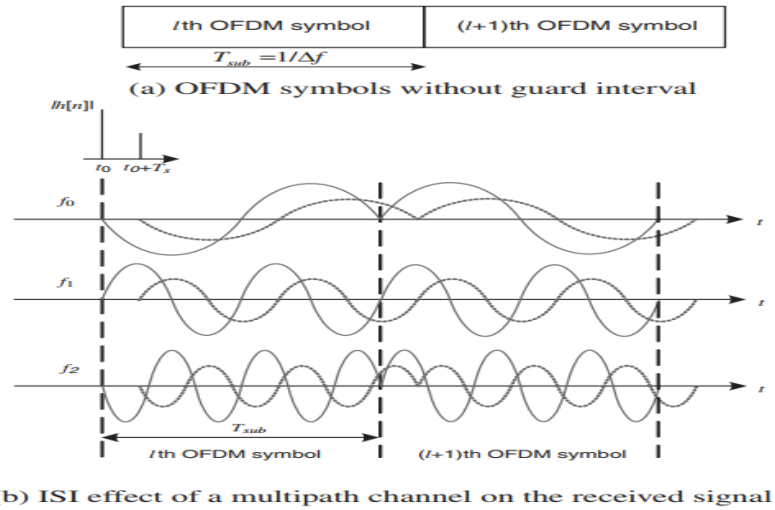

Figure 1-7: Effect of a multipath channel on the received signal without guard interval

As shown in Figure 1-7 (b), the first received symbol (plotted in a solid line) is mixed up with the second received symbol (plotted in a dotted line), which incurs the ISI. It is obvious that all subcarriers are no longer orthogonal over the duration of each OFDM symbol. To warrant a performance of OFDM, there must be some means of dealing with the ISI effect over the multipath channel. As discussed in the sequel, a guard interval between two consecutive OFDM symbols will be essential.

The OFDM guard interval can be inserted in two different ways. One is the zero padding (ZP) that pads the guard interval with zeros. The other is the cyclic extension of the OFDM symbol (for some continuity) with CS (cyclic suffix) or CP (cyclic prefix). [Yon10]

1.4.2.4.2. Cyclic Prefix (CP):

CP is to extend the OFDM symbol by copying the last samples of the OFDM symbol into its front. Let T_G denote the length of CP in terms of samples. Then, the extended OFDM symbols now have the duration of $T_{sym} = T_{sub}+T_G$.

Figure 1-8 (a), shows two consecutive OFDM symbols, each of which has the CP of length T_G, while illustrating the OFDM symbol of length $T_{sym} = T_{sub}+T_G$. Meanwhile, Figure 1-8 (b), illustrates them jointly in the time and frequency domains. [**Yon10**]

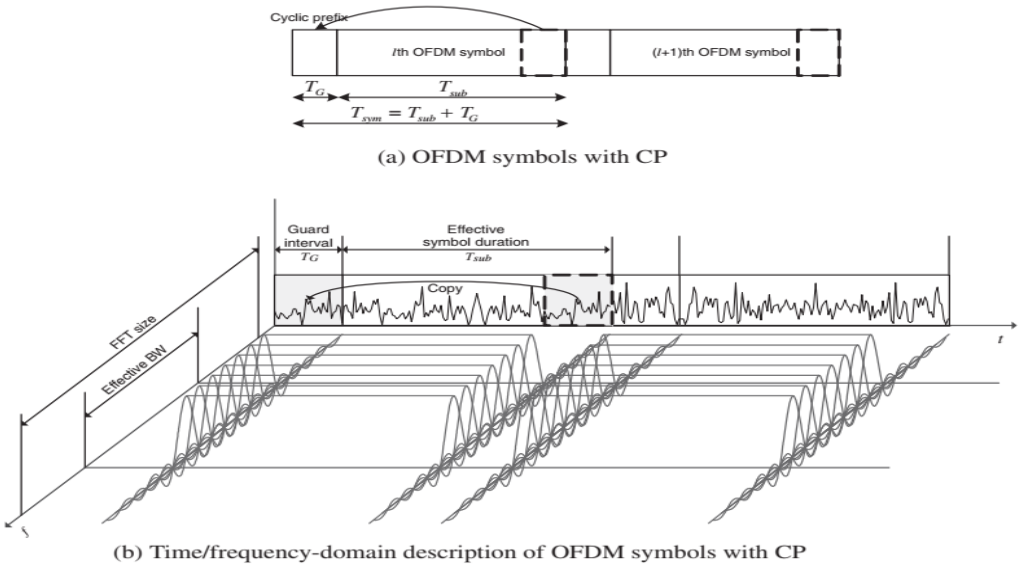

(a) OFDM symbols with CP

(b) Time/frequency-domain description of OFDM symbols with CP

Figure 1-8: Use of CP in OFDM symbols

1.4.2.4.3. Cyclic Suffix (CS):

A cyclic extension of the OFDM scheme depicts a cyclic suffix (CS). the CS is the duplicate of the head part of an effective OFDM symbol and adds it to the end of the symbol. CS is used to stop upstream and downstream interference and is often used as the guard interval for frequency hopping or convergence of RF, and so on. In Zipper-based VDSL (Very high-speed digital subscriber line systems), both CP and CS are used in which the Zipper duplexing technique is a type of FDD (Frequency Division Duplexing) allocating different frequency bands (subcarriers) to downstream or upstream transmission, in an OFDM symbol that allows simultaneous bidirectional signal flow. Here, CP and CS are intended to suppress the multipath channel's ISI effect, thus securing the orthogonality between the signals upstream

and downstream. The CP length is indeed set to cover the channel's time dispersion, while the CS length is set according to the difference between the time of upstream transmission and the time of downstream reception. The structure of the OFDM symbol used in Zipper-based VDSL systems is shown in Figure 1-9, where the length of the guard interval is the sum of CP length TCP and CS length TCS [**Yon10**]

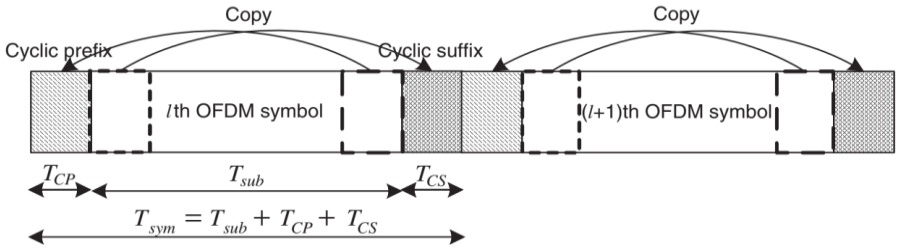

Figure 1-9: OFDM symbols with CS &CP

1.4.2.4.4. Zero Padding (ZP):

Into the guard interval, we can insert zero. In an Ultra Wide-band (UWB) system, this particular approach is adopted by multiband OFDM (MB-OFDM). A small Shift Time Offset (STO) causes the OFDM symbol of an effective duration to have a discontinuity within the FFT window even with the length of ZP longer than the maximum delay of the multipath channel, so the guard interval part of the next OFDM symbol is copied and applied to the head part of the current symbol to avoid ICI as defined in Figure 1.11.

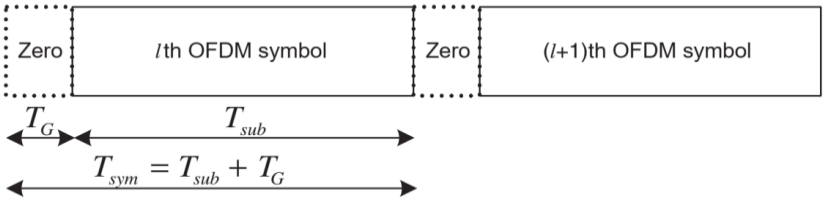

Figure 1-10: OFDM symbols with ZP.

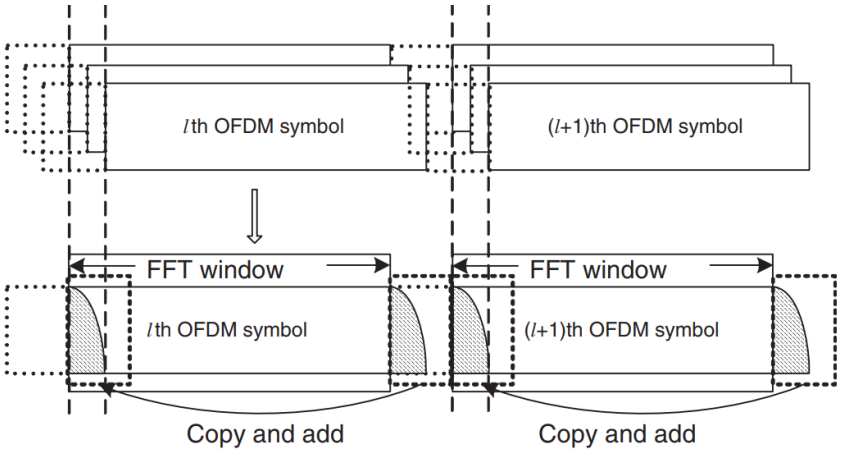

Figure 1-11: Copying-and-adding the guard interval of the next symbol into the head part of the current symbol to prevent ICI.

Since the ZP is filled with zeros, the actual length of an OFDM symbol containing ZP is shorter than that of an OFDM symbol containing CP or CS and accordingly, the length of a rectangular window for transmission is also shorter, so that the corresponding sinc-type spectrum may be wider. This implies that compared with an OFDM symbol containing CP or CS, an OFDM symbol containing ZP has PSD (Power Spectral Density) with the smaller in-band ripple and the larger out-of-band power as depicted in Figure 1.12, allowing more power to be used for transmission with the peak transmission power fixed. [**Yon10**]

Note that the data rate of the OFDM symbol is reduced by $T_{sub}/T_{sym}=T_{sub}/(T_{sub}+T_G)$ times due to the guard interval.

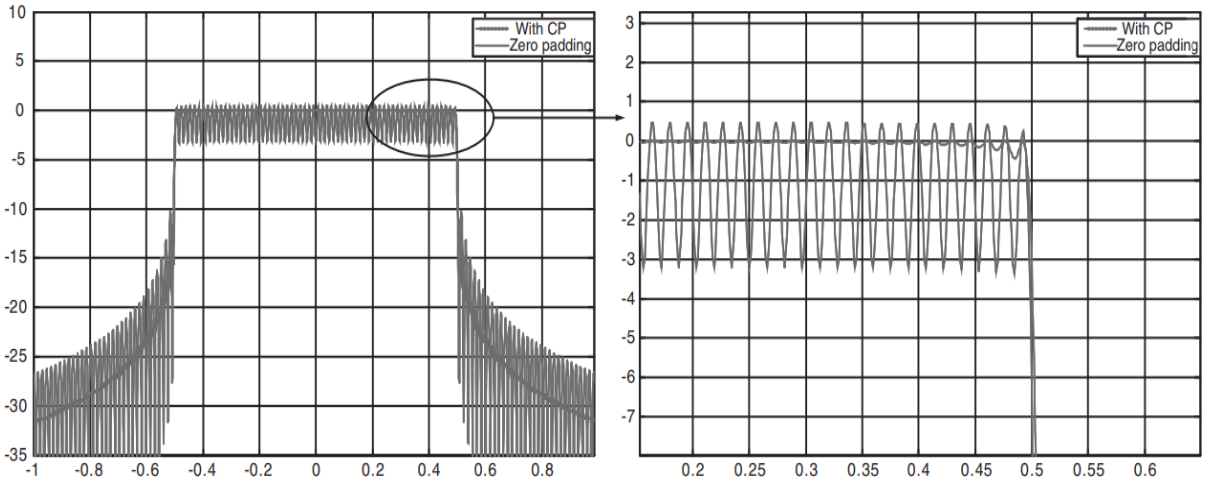

Figure 1-12: Power spectra of two OFDM symbols, one with ZP and one with CP.

1.4.2.4.5. OFDM Guard Interval advantages and disadvantages:

There are several advantages and disadvantages attached to the use for the OFDM Guard Interval within OFDM.

a. Advantages:

- *Provides robustness:* The addition of the cyclic prefix adds robustness to the OFDM signal. The data that is retransmitted can be used if required.
- *Reduces inter-symbol interference*: The guard interval introduced by the cyclic prefix enables the effects of inter-symbol interference to be reduced.

b. Disadvantages:

- *Reduces data capacity:* As the cyclic prefix re-transmits data that is already being transmitted, it takes up system capacity and reduces the overall data rate.

So, the use of a Guard Interval is standard within OFDM and it enables the performance to be maintained even under conditions when levels of reflections and multipath propagation are high.

1.4.2.5. OFDM Guard Band:

Each OFDM symbol subcarrier portion with the effective $\boldsymbol{T_{sub}}$ duration can be regarded as a single-tone signal multiplied by a rectangular $\boldsymbol{T_{sub}}$ length window, whose spectrum is a sinc function with a $\boldsymbol{2/T_{sub}}$ zero-crossing bandwidth. The power spectrum of an OFDM signal is therefore the sum of several frequency-shifted sinc functions, which have a significant out-of-band power that is incurred by ACI (adjacent channel interference). As a consequence, in order to reduce the effect of ACI on the OFDM system, a guard band is required.

A Base Pass Filter (BPF) can be used to minimize the out-of-band power of OFDM symbols, but to make the filtering efficiency appropriate, it may require enormous computation and high complexity. A time-domain shaping feature like raised cosine (RC) windowing can be used as an option. The use of virtual carriers (VCs), which are the unused subcarriers at both ends of the transmission band, is another step against the ACI. When the virtual carriers are hired, no extra processing is needed. However, due to the unused subcarriers, the spectral (bandwidth) efficiency is decreased by $\boldsymbol{N_{used}/N}$ times, where $\boldsymbol{N_{used}}$ is the number of subcarriers used for data transmission. In combination with the (RC) window, the virtual carriers can be used to decrease the out-of-band power and eventually battle the ACI. [**Yon10**]

1.4.2.6. Equalization:

Equalizer is a filter that mitigates the effects of channel fading on the Rx signal and removes the Inter-Symbol Interference (ISI). Equalization in OFDM systems is performed in the frequency domain. This is simpler than the time domain equalization which is normally employed in single carrier systems. Time domain equalization increases rapidly in complexity with the increase in data rate. Whereas, frequency domain equalization remains relatively simple and easy to implement.

1.4.3. OFDM advantages and disadvantages:

1.4.3.1. OFDM advantages:

OFDM has been used in many high data rate communication systems because of the many advantages it provides.

- Immunity to selective fading: One of the main advantages of OFDM is that is more resistant to frequency selective fading than single carrier systems because it divides the overall channel into multiple narrowband signals that are affected individually as flat fading sub-channels.
- Resilience to interference: Interference appearing on a channel may be bandwidth limited and in this way will not affect all the sub-channels. This means that not all the data is lost.
- Spectrum efficiency: Using close-spaced overlapping sub-carriers, a significant OFDM advantage is that it makes efficient use of the available spectrum.
- Resilient to ISI: Another advantage of OFDM is that it is very resilient to inter-symbol and inter-frame interference. This results from the low data rate on each of the sub-channels.

- Resilient to narrow-band effects: Using adequate channel coding and interleaving it is possible to recover symbols lost due to the frequency selectivity of the channel and narrow band interference. Not all the data is lost.
- Simpler channel equalisation: One of the issues with CDMA systems was the complexity of the channel equalisation which had to be applied across the whole channel. An advantage of OFDM is that using multiple sub-channels, the channel equalization becomes much simpler.

1.4.3.2. OFDM disadvantages:

Whilst OFDM has been widely used, there are still a few disadvantages to its use which need to be addressed when considering its use

- High peak to average power ratio: An OFDM signal has a noise like amplitude variation and has a relatively high large dynamic range, or peak to average power ratio. This impacts the RF amplifier efficiency as the amplifiers need to be linear and accommodate the large amplitude variations and these factors mean the amplifier cannot operate with a high efficiency level.
- Sensitive to carrier offset and drift: Another disadvantage of OFDM is that is sensitive to carrier frequency offset and drift. Single carrier systems are less sensitive.
- High synchronism accuracy.
- More complex than single-carrier Modulation.
- Requires a more linear power amplifier.
- Bandwidth and power loss due to the guard interval can be significant.

1.4.4. Applications of OFDM:

Orthogonal frequency-division multiplexing (OFDM) as a technology that enables robust transmission over both wireless and optical channels has already been employed in many communication standards such as:

1.4.4.1. Mobile WIMAX:

Worldwide Interoperability for Microwave Access (WIMAX) uses orthogonal frequency division multiple access (OFDM) as a multiple-access technique, whereby different users can be allocated different subsets of the OFDM tones.

1.4.4.2. LTE:

To overcome the effect of multi path fading problem available in UMTS, LTE (Long-Term Evolution) uses Orthogonal Frequency Division Multiplexing (OFDM) for the downlink that is, from the base station to the terminal to transmit the data over many narrow band careers of 180 KHz each instead of spreading one signal over the complete 5MHz career bandwidth. OFDM uses a large number of narrow sub-carriers for multi-carrier transmission to carry data. OFDM meets the LTE requirement for spectrum flexibility and enables cost-efficient solutions for very wide carriers with high peak rates. The basic LTE downlink physical resource can be seen as a time-frequency grid, as illustrated in Figure 1-12 below

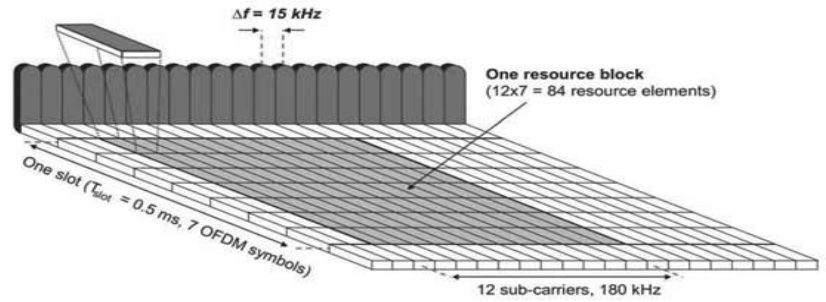

Figure 1-13: Frequency-Time grid of an OFDM signal.

The OFDM symbols are grouped into resource blocks. The resource blocks have a total size of 180 kHz in the frequency domain and 0.5ms in the time domain. Each 1ms Transmission Time Interval (TTI) consists of two slots (T slot), each user is allocated a number of so-called resource blocks in the time/frequency grid. [**Wiki**]

1.4.4.3. DVB-T:

The DVB-T (digital video broadcasting-terrestrial) Orthogonal Frequency Division Multiplexing modulation system uses multi-carrier transmission. There are 2 modes, the so-called 2k and 8k modes, using 1705 and 6817 carriers respectively, with each carrier modulated separately and transmitted in the 8 MHz TV channel.

1.4.4.4. DAB:

DAB (Digital audio broadcasting) is a radio system which is depends on EUREKA-147 project. This project was designed by the Members of European Broadcasting Union (EBU). DAB System depends on wireless communication. DAB channel estimation was designed by the OFDM technology that reduces co-channel interference and multipath fading.

1.4.4.5. Wireless ATM transmission system:

An orthogonal frequency division multiplexing (OFDM)-based wireless ATM (asynchronous transfer mode) transmission system is described that is suitable for the future broad-band mobile multimedia communications. In the proposed system, guard symbols, which are cyclically extended by repeating the information symbols, are inserted before and after serial-to-parallel converted wireless ATM data symbols for OFDM transmission. These symbols are used for both wireless ATM frame synchronization and deciding the discrete Fourier transformation (DFT) start point at the receiver. A cyclically extended pseudorandom noise (PN) sequence is inserted into some of the OFDM transmission subchannels at fixed intervals and used to estimate the phase rotation, frequency offset, and delay characteristics. The proposed system does not use "symbol-by-symbol" guard-interval insertion or removal circuits, as do conventional OFDM systems. With this system, it is easy to estimate the phase rotation, frequency offset, and delay characteristics and to synchronize wireless ATM cells. Computer simulation showed that the bit error rate (BER) performance of the proposed system is better than that of a conventional "symbol-by-symbol" OFDM system. [**Wiki**]

1.4.4.6. ADSL:

OFDM is used in ADSL (Asymmetric Digital Subscriber Line) connections, where it is called discrete multitone modulation (DMT). The basic idea of DMT is to split the available bandwidth into 256 bands or subchannels. DMT is able to allocate data so that the throughput of every single subchannel is maximized. If some subchannel can't carry any data, it can be turned off and the use of available bandwidth is optimized.
OFDM is also used in the successor standards ADSL2, ADSL2, VDSL, VDSL2, and G.fast VDSL uses variable subcarrier modulation, ranging from BPSK to 32768QAM.

1.4.4.7. LI-FI:

The use of OFDM allows for further adaptive bit and power loading techniques on each subcarrier so that enhanced system performance can be achieved. The OFDM generated signal is complex and bipolar by nature. In order to fit the LEDs functions requirements, necessary modifications to the conventional OFDM techniques are needed for Li-Fi (Light-Fidelity).

1.5. Conclusion:

The demand for high data rate wireless communication has been increasing drastically over the last decade. One way to transmit this high data rate information is to employ well-known conventional single carrier systems. Since the transmission bandwidth is much larger than the coherence bandwidth of the channel, highly complex equalizers are needed at the receiver for accurately recovering the transmitted information. Multi-carrier techniques can solve this problem significantly. In this part we have discussed about the basic idea behind the OFDM, the most emerging technology of this era. Here we took a review on its concept, its properties in terms of its advantages and disadvantages, its limitations and also its applications in different fields. Also, we had explored the role of OFDM in the wireless communication and its advantages over single carrier transmission.

Chapter 2:

Visible light communication

2.1. Introduction:

Optical communication is an important part of modern communication techniques due to the excessive bandwidth of the light spectrum. Theoretically, optical communication has much higher system throughput than its radio frequency (RF) communication counterpart. Therefore, it finds many applications and facilitates our lives. Some typical optical communication scenarios include optical fiber communication, free-space optical communication, and visible light communication. In those communication scenarios, intensity modulation and direct detection (IM/DD) is a cost-effective communication scheme compared to coherent ones. In IM/DD, the intensity, or power, of the light beam from a laser or a light-emitting diode (LED) is modulated by the information bits and no phase information is needed. Due to this nature, no local oscillator is required for IM/DD communication, which greatly eases the cost of the hardware.

In IM/DD channel, the multipath effects and the limited modulation bandwidth of LED. Thus, introducing OFDM to IM/DD optical communication is a natural choice.

The purpose of this chapter was to study the Optical Wireless Communication specially the Visible Light Communication (VLC) system and analyse the potential forms of OFDM that are suitable for IM/DD transmission as well as VLC weak-points of this system.

2.2. General Context of Optical Wireless Communication Systems and Technologies:

wireless networking has quickly developed after the discovery of electromagnetic (EM) waves. From the creation of the invention of radio to the cellular telephone, it has seen several paradigm changes. Today, because of a major rise in the introduction of wireless networks, there has been a widespread presence of wireless applications and machines. Soon, applications such as music, web browsing, video telephony, television, virtual reality, video streaming in high definition (HD) would require high bandwidth and high data rates to meet the demands. More than 30 billion connected devices will also be related to a major interest in the Internet of Things (IoT) by 2020. At the same time, the demand for universal mobility and communication access is rising exponentially as network traffic statistics study projected by Cisco global, shown in Figure 2-1. It can be observed that worldwide network traffic is rising steadily at a rapid rate, and this estimated global network traffic inflation is expected to prevail over the next few years. Some significant Cisco predictions are:

- there shall be 3.5 network devices and connections per person by 2021;
- the average internet traffic per person per month will be 61 GB by 2021;
- there shall be 4.6 billion internet users with 27.1 billion network devices and connections around the globe by 2021.

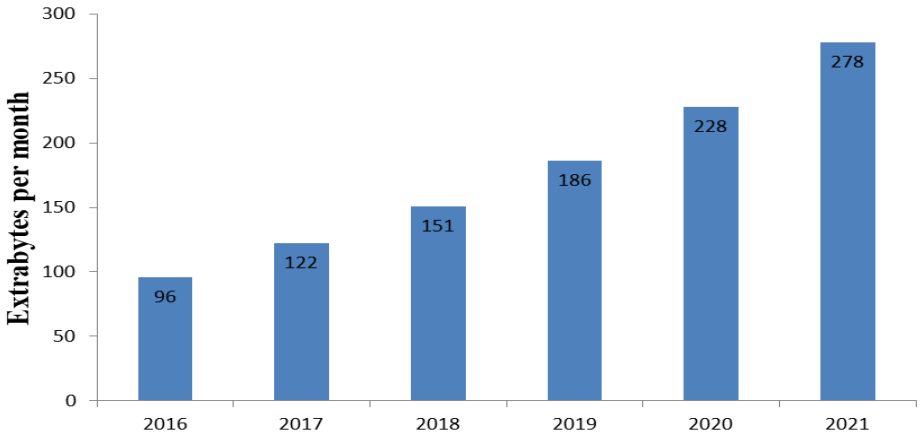

Figure 2-1: Global visual network Index predictions.

For radio-frequency (RF) technologies, the word 'wireless' is commonly called, since most of the technologies in use are focused on RF devices and systems. The 3 kHz to 300 GHz RF spectrum is a natural resource exclusively regulated and managed by the state that appropriates rights and optimizes the use of the spectrum. RF spectrum is required for many applications, such as analog and digital radio broadcasting, television (TV) broadcasting, radar, satellite communications, mobile communications, wireless local area networks (WLANs), various government, industrial and public applications, etc. With the inflated demand for data-hungry wireless applications over the last couple of decades, a massive amount of RF bandwidth is being consumed. Most of the RF spectrum has been reserved and spectral congestion might be triggered by the current pattern.

This challenge will cause a negative impact and leave behind a substantial gap between prevailing systems' deliverable capacity and the demands for exponentially growing network traffic. Global network traffic grew roughly 18 times between 2011-2016, affirming that spectrum shortage is becoming a reality. Spectral control is therefore crucial to evade spectral exhaustion. Different approaches have been proposed to tackle this issue, some leading solutions are:

- With the current structures, the first solution is to be spectrally more efficient. For the last decade, this has been achieved by implementing techniques such as multiple-input and multiple-output (MIMO), which increase the ability of the device. These methods aim to increase the spectral efficiency of bits /s/Hz, but this solution is approaching saturation.
- One other strategy is to be more vigorous by reusing the spectrum temporally and spatially. The use of cognitive radio, where the spectrum is dynamically distributed to prevent interference between different users and to avoid congestion, are exploited in this solution. Further, there is a principle of off-loading in which a high density of small cells are employed by scaling down the cell coverage area. The definition of femtocells and attocells is examined in this regard, but increased interference between the access nodes is one demerit of this approach. The aim of these methods is to boost bits /s/Hz/m2.
- The third technique is to use portions of the spectrum that are not typically used for communication purposes. The definition of millimetre wave (mm-Wave)

communications has gained significant interest in this context. The unconventional portions of the 28 GHz to 250 GHz spectrum are used for communication purposes in mm-Wave communications. Using massive MIMO technology that makes several small antennas within an area because of shorter wavelengths which its wave propagation is limited to only line-of-sight (LoS) scenarios and thus surrenders the widespread coverage advantage over RF. The absence of high bandwidth / low power consumption mm-Wave transceivers for high frequencies is another potential drawback for mm-Wave systems. A large part of the current infrastructure needs to be replaced in order to use such systems. Terahertz (THz) communication systems are also explored as an option that can deliver a wide range from 1000 GHz to 3000 GHz, but the key problem is the THz transmitter and receiver implementation.

In addition to the 3 kHz to 300 GHz RF spectrum, there is an optical spectrum consisting of the infrared (IR), visible light (VL) and ultraviolet (UV) spectrum, ranging from 300 GHz to 30 petahertz (PHz), as shown in Figure 2-2. This optical spectrum can be used for communication primarily because of enormous un-regulated, un-licensed bandwidth which can provide high data-rates and can be a potential solution for the last mile problem. The optical spectrum, thousands of times wider than the RF spectrum, is used for optical wireless communication (OWC). The OWC systems, however, have their own problems, such as decreased sensitivity due to obstacles and insufficient transmitted optical capacity, etc.

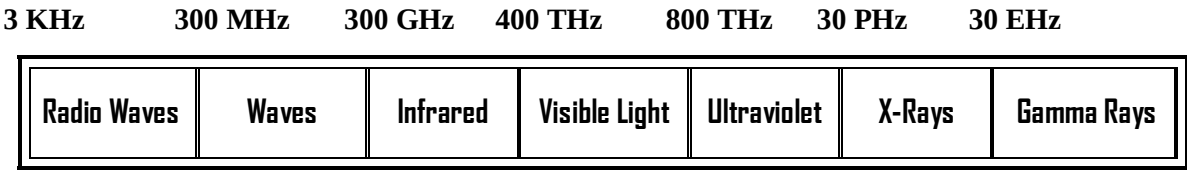

Figure 2-2: The electromagnetic (EM) spectrum.

In OWC, the message can be transmitted via the methods of intensity modulation and direct detection (IM-DD) in which the data is modulated on the electromagnetic radiation envelope that is photodetected at the receiver. IM-DD is based on the use of electrical-to-optical transceivers, such as transmitter light emitting diodes (LEDs) and laser diodes (LDs), and optical-to-electrical transceivers such as receiver photo-diodes (PDs). In addition to the availability of the immense unregulated spectrum available for OWC, the following section offers some other driving factors as to why OWC is used. [**Ali18**]

2.2.1. Motivations for Optical Wireless Communications:

OWC technologies are seen as a possible solution to the issue of the last mile and can close the gap between end users and the backbone networks of the optical fiber. The interest in using OWC is motivated by the following considerations:

- *Energy Efficiency:* As the energy used for lighting (for visible light communications (VLC)) can also be used for communication, an OWC device does not need exclusive energy resources. In addition, relative to other lighting sources, LEDs used for VLC are more energy efficient and have a slightly lower carbon dioxide (CO2) footprint,

which may contribute to green communication technology. CO2 emissions are projected to be decreased by 10 Giga-tons by replacing current lighting with LEDs, which decreases oil consumption by 962 million barrels, which will lead to cost savings of trillions of dollars and energy savings of 1.9x1020 joules over a decade.

- *Data Security:* In comparison to RF waves, the snooping can be avoided, the light intensity signal used for OWC cannot penetrate through the walls or any other obstacles that make them a safer communication choice. In addition, in the area surrounded by opaque borders, the light intensity signal is limited, so all contact occurring within the room remains in the room, which is not possible with RF waves.
- *Safety:* The use of luminaries for OWC have no apparent health hazards and conform with the eye-and-skin safety regulations making it safe in practical communication scenarios.
- *Interferences:* The use of light intensity signal for OWC is intrinsically safe and offers zero interference with RF signals or RF sensitive equipment. Therefore, this technology is safe to use in places where RF signals are restricted or not allowed due to interferences with RF sensitive equipment, such as hospitals and aerospace platforms.
- *Spatial Reuse and Beam Steering:* In indoor OWC systems, the light intensity signal is confined due to reflections from walls, roof and ceiling. Hence, this highly confined and directed light beam makes it possible to create multiple non-interfering beams in close proximity. This allows greater data density and reuse of modulation bandwidth in adjacent cells. Additionally, unlike RF wireless technologies which need complex and costly equipment for beam steering, light can be easily directed using low-cost optical equipment.
- *Easy Integration to Existing Infrastructure and Hardware Reuse:* The incorporation of OWC systems into the current infrastructure is very easy since only low-cost front-end modules, such as LEDs and related drivers, such as PDs and related amplification phases, need to be installed. The current lighting infrastructure intended for lighting can be leveraged to incorporate communications for indoor OWC systems and the initial set-up costs of an entire new system can be avoided. RF/mm-Wave and THz communications, on the other hand, need to plan, assemble and deploy dedicated, complicated transceivers that can increase integration costs.
- *Low Recurring Cost:* The components used for OWC impose very low recurring costs because: I they are typically energy efficient, resulting in low billing costs; (ii) no specialized wireless transmission equipment is needed unlike RF, reducing the fuel cost of maintaining the RF base stations in working order. As an example, RF connections in the 2.4 GHz band with the transmission distance and rate of 10 m and 1 Mbps incur a cost of almost 5 US dollars, while OWC is able to achieve 4 Mbps over short distances and cost around 1 US dollar. [**Ali18**]

2.2.2. Applications of Optical Wireless Communications:

OWC has a broad variety of possible uses. The graphical overview of possible OWC application platforms is given in Figure 2-3. Airports, petrochemical plants, smart homes and towns, train stations, healthcare, data centers, transport, underwater communication, etc. are some prospective application platforms. Diverse communication methods can be incorporated within these networks, such as chip-to-chip (C2C), device-to - device (D2D) and machine-to-machine (M2 M). And then, in creating IoT, where millions of smart devices could be related to each other, these techniques can be invaluable.

In such platforms, OWC can be more effective, where RF signals can interact with other sensitive facilities, such as hospitals / healthcare and petrochemical plants, etc. The reliable communications strategy for military submarines, where internal communications can be formed in a silent mode, is another example of OWC. Contact distance is one fundamental consideration that is needed for the implementation of OWC technologies. OWC implementations can be categorized into ultra-short range, short range, medium range, long range and ultra-long range on the basis of contact distance, as shown in Figure 2-4. This means that OWC applications, as shown in Figure 2-5, range from C2C communications at a distance of a few micro-meters to inter-satellite and deep space connections at distances of thousands of kilometres. Few examples follow:

- *Ultra-Short Range OWC Applications*: Due to high bandwidth and low latency, optical interconnects are gaining significant importance and are expected to eliminate copper-based electrical interconnects that are bulky and prove to be a bottleneck in device design. For C2C contact, OWC may be used in optical interconnections, which can be a flexible, less cumbersome alternative for conventional electrical wire equivalents.

Figure 2-3: Potential applications of OWC

- *Short Range OWC Applications:* Typical examples may be wireless body area network (WBAN) and wireless personal area network (WPAN) for short range OWC in the order of tens of centimeters. Many sensors/detectors can be mounted on the

body in WBANs to monitor the parameters of health, such as heart rate, blood pressure, etc. RF signal-based WBAN might not be a good choice for hospitals where the equipment is sensitive to RF signals. In OWC-based WBANs, VL-based sensors can be inserted into clothing or wearable devices that can capture critical information from a smartphone. In WPAN, the key principle of IoT is that all devices gathered around a person are connected to each other.

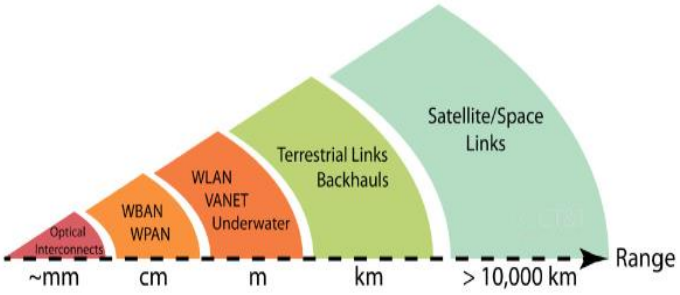

Figure 2-4: Categorization of OWC applications based on the transmission range

- *Medium Range OWC Applications*: WLANs are a popular application of OWC for minimum transmission distances. RF wireless connections are typically used, however, as described above, RF spectrum is practically exhausted accordingly, OWC may be a potential replacement. With the idea of using LEDs for both lighting and communication, the creation of WLANs using OWC can become a reality for inter-building wireless connectivity. For outdoor situations, such as traffic lights, street lamps, marketing shows, vehicle headlights / taillights, VLC may also be used. This can result in the contact of vehicle-to-infrastructure (V2X), vehicle-to-vehicle (V2V).

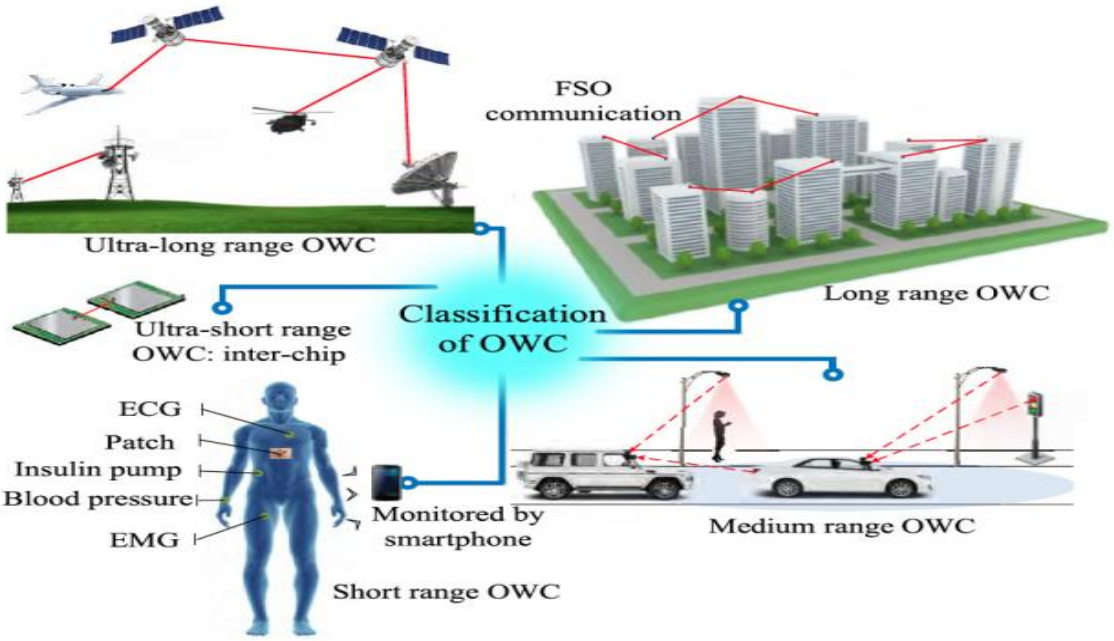

Figure 2-5: OWC application classification based on communication distance.

- *Long Range OWC Applications:* OWC can be used to link one WLAN to another WLAN for long-range applications. Free space optics (FSO) networks have high Tbps-ordered bandwidth, high data rates and are easy to reconfigure. In conventional coaxial cables, long-range OWC ties can be used as backhaul connections to surmount the bottleneck. Nowadays, optical free-space connections are also used for aerospace applications.
- *Ultra-Long Range OWC Applications:* Free space optic connections can be a effective means of communication for distances of thousands of kilometers, such as ground-to-satellite and inter-satellite communications. Several inter-satellite free space optic connections have been explored, demonstrating the ability of OWC for long-range FSO applications, for example.

Visible light communication (VLC), light fidelity (LiFi), optical camera communications (OCC) and free space optics (FSO) are various envisioned technologies for OWC. These technologies are mainly distinguished by the type of receiver or the optical spectrum area that they use. [**Ali18**]

2.3. Visible Light Communication (VLC):

Within the subset of OWC, there is a considerable interest in VLC. VLC, as the name It is an OWC technology that uses the VL spectrum. VLC is intended to be a complementary technology to the prevalent RF systems and to be able to fulfill IoT requirements. VLC may, however, function within restricted transmission ranges. Without the limitation of minimal available spectral bandwidth, it can be used for different applications in houses, automobiles, aerospace, trains etc. The high prevalence of LEDs makes it easy to deploy VLC. LEDs can turn easily, indistinguishable to the human eye, between different intensities. In addition, of course, the light produced by LEDs used for lighting purposes is harmless to humans. The current lighting infrastructure can be used for VLC, as LEDs can be used for communication. By using LEDs many VLC applications can be assured as data-rates of up to 10 Gbps, smart lighting, smart cities, wireless networking, use in RF-sensitive environments, indoor localization, virtual reality, ete.

A VLC system mainly consists of a VLC transmitter that modulates the light emitted by LEDs and a VLC receiver centred on a photosensitive element (photodiode) that is used to extract the modulated signal from the light. Physically, the transmitter and the receiver are isolated from each other, but linked through the VLC channel. The Line of Sight (LoS) is a required factor for VLC systems. [**Ali18**]

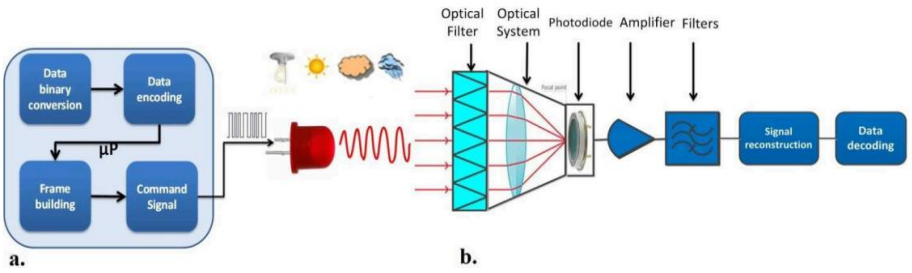

Figure 2-6: Schematic of a VLC system.

2.3.1. Optical Sources and Detectors:

The most commonly used optical sources and detectors are the incoherent sources-light emitting diodes and photodetectors, respectively. In this section the basic properties of LEDs and photodetectors are discussed.

2.3.1.1. Basic Properties of LED:

The LED is a semiconductor p-n junction device that causes current to flow and produces optical radiation by spontaneous emission through the application of a forward bias voltage across the device. The theory, demonstrated in Figure 2-7, is the following: electrons pass to a p-n junction region in the n-type and p-type holes and recombine with an opposite polarity region. Electrons and holes will recombine in two different ways during the recombination process: radiatively and non-radiatively.

The electron returning to the valence band gives off its energy as a photon during the radiative recombination. Phonons (heat) are only given out by non-radiative recombination.

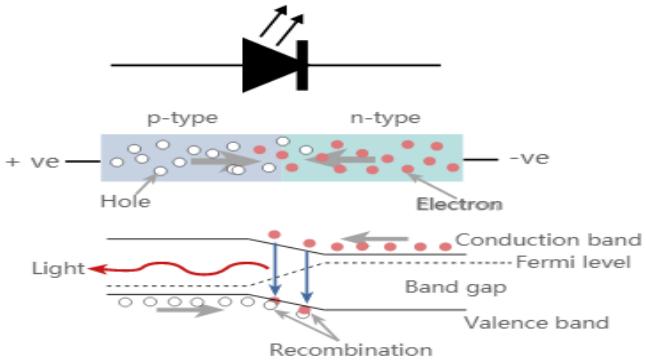

Figure 2-7: Forward bias condition operation in an LED.

The wavelength of the emitted photons $\boldsymbol{\lambda}$ is directly associated with the semiconductor material's ($\boldsymbol{\lambda\, \alpha\, E_g}$) energy band-gap $\boldsymbol{E_g}$, which has an effect on the threshold voltage $\boldsymbol{V_{th}}$. Both wavelength of the emitted photons and threshold voltage can be expressed as

$$\boldsymbol{\lambda = \frac{hc}{E_g}} \tag{2.1}$$

$$\boldsymbol{V_{th} = \frac{E_g}{q}} \tag{2.2}$$

where $\boldsymbol{h}$ is the Planck constant, $\boldsymbol{c}$ is the speed of light and $\boldsymbol{q}$ is the electron charge constant. In the Shockley equation, the diode current, $\boldsymbol{I_D}$ is expressed as a function of the applied voltage $\boldsymbol{V}$, thus explaining the current-voltage characteristic of the LED as described further. The Shockley equation is given as

$$\boldsymbol{I_D = I_s(e^{\frac{q(V-V_{th})}{kT}} - 1) \rightarrow I_D \alpha P_{optical}} \tag{2.3}$$

Where the reverse bias saturation current expressed by $\boldsymbol{I_s}$, $\boldsymbol{K}$ is the constant of Boltzmann, $\boldsymbol{T}$ is the temperature of the device and $\boldsymbol{P_{optical}}$ is the optical power. From equation (2.3), the current increases rapidly as the voltage $\boldsymbol{V}$ reaches $\boldsymbol{V_{th}}$ under the forward bias condition due to the exponential component. As the voltage across the device is proportional to the current, more electrons recombine as the voltage rises, leading to higher emission of photons (higher radiated optical power $\boldsymbol{P_{optical}}$). As current increases, the properties of the LED become nonlinear, causing distortions. The LED size is inversely proportional to the bit rate and the higher number of LEDs in a different wavelength transmission system results in higher data transmission. An LED's modulation bandwidth depends on the injected current, the capacitance of the junction, and the parasitic capacitance. The relative optical power output at any frequency given is expressed as

$$\frac{\boldsymbol{P_{(w)}}}{\boldsymbol{P_0}} = \frac{\mathbf{1}}{\sqrt{\mathbf{1} + (\boldsymbol{w\tau})^2}} \tag{2.4}$$

where $\boldsymbol{P_{(w)}}$ is the power at frequency $\boldsymbol{w}$, $\boldsymbol{P_0}$ the DC power and $\boldsymbol{\tau}$ the spontaneous recombination lifetime including both radiative and non-radiative recombination. By setting equation (2.4) to 0.5, the -3 dB bandwidth is obtained which is defined from 0 Hz to the frequency transmitted by the LED. An LED dedicated for communication purposes has a smaller active region, thus a smaller RC time constant, which implies a higher bandwidth and faster modulation processes.

Communication systems typically suffer from non-linearity introduced by out-of-band radiation caused by electronic components. This leads to a decrease in spectral efficiency and distortion of the in-band, generating ICI and degrading the output of errors. Because of its non-linear transfer feature, which may distort the OFDM signal, the LED is one of the key impairments affecting the output of a VLC device.

As shown in figure 2-8, the non-linear transfer characteristic of an LED can be defined as the non-linear relationship between the forward current and the forward voltage. The LED has a threshold value known as a turn-on voltage where the LED is considered in a cut-off region and does not conduct current at any value below that point. The current and the output amplitude rise exponentially with the voltage above the turn-on voltage until the current begins to saturate. Due to the nonlinear feature of an LED, high PAPR input signals in an IM / DD device can suffer from distortion due to clipping.

A research was done where, the LED can operate around a bias point in a quasi-linear segment of its features through DCO-OFDM, thus regulating the levels of distortion. The biasing point should maximize the forward current that is acceptable and eliminate signal clipping and distortion of magnitude. In addition, by running the LED in a quasi-linear segment around the bias point, signal power back-offs can be used to reduce distortion levels. The OFDM signal therefore modulates around a certain DC bias point known as the bias voltage $\boldsymbol{V_{bias}}$. [**Ped18**]

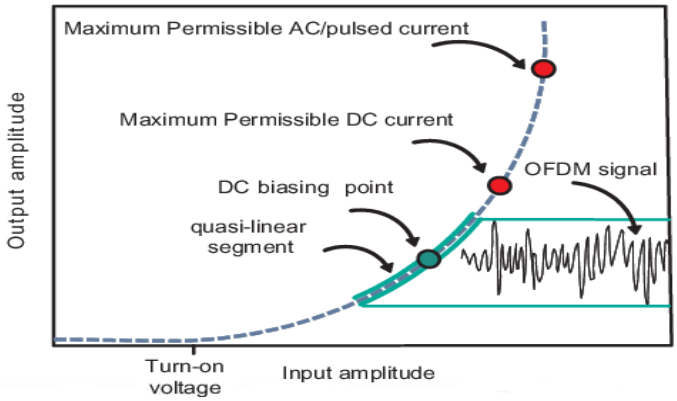

Figure 2-8: Non-linear LED characteristics.

2.3.1.2. Basic Properties of a Photodetector:

A photodetector is a square-law [2] optoelectronic transducer that converts an optical signal into an electric current. Since the electric current generated by the photodetector is proportional to the received optical signal, and generally this optical signal is weak (having travelled through the communication channel), the photodetector must meet strict performance requirements such as high sensitivity and responsivity around operating wavelengths, low noise (thus higher SNR) and an adequate bandwidth to accommodate the desired data rate. When incident photons with a greater energy than the semiconductor band-gap are absorbed, it generates electron-hole pairs. However, when the energy of incident photons is smaller than the band-gap the incident photons cannot be absorbed and the semiconductor appears transparent. The ratio of the number of electron-hole pairs generated by a photodetector to the incident photons in a given time is defined as quantum efficiency, which can be approximated by

$$\eta_{qe=}\xi(1-R_{ref})(1-e^{\alpha d}) \tag{2.5}$$

where ξ is the ratio of electron-hole pairs leading to the photocurrent, R_{ref} is the optical reflection coefficient, d is the distance where optical power is absorbed and α is the optical absorption coefficient.

The latter will impact the photodetector structure by determining the penetration depth of the light in the semiconductor material contributing to its responsivity. The responsivity of a photodetector is defined as the photocurrent generated per unit incident optical power, in other words, it translates to the light-to-current conversion efficiency. Considering an ideal photodetector where $\xi = 1$, the responsivity is expressed as

$$R = \frac{I_{ph}}{P_{inc}} = \frac{\lambda[\mu m]q}{hc}\eta_{qe} \tag{2.6}$$

[2] **A square-law device has output signal values proportional to the square of the input signal values, in case of a photodetector the square of the electric field ($|E|2$).**

where I_{ph} is the photocurrent and P_{inc} in the incident optical power. A highly responsive photodetector means a higher photocurrent generated from a given incident optical power. An ideal photodetector is not feasible, in general the responsivity of a real photodetector is lower due to partial reflection of the light at the semiconductor surface as well as partial recombination of photogenerated carriers in the semiconductor or at its surface. The difference between the responsivity of an ideal and real photodetector is illustrated in figure 2-9, which can be explained by the difference in values of η_{qe} in equation (2.6). [**Ped18**]

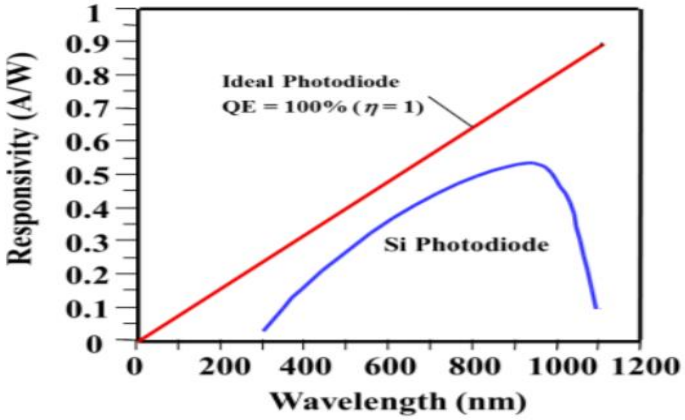

Figure 2-9: Differences in responsivity of an ideal vs. real typical silicon photodetector.

2.3.1.3. Basis of Photometry:

In comparison to radiometry, which defines the detector-independent measurement of electromagnetic radiation, photometry is the science of light measurement in which the detector represents the reaction of the human eye system. To better understand the concept of VLC systems, the basic principles of photometry are added, including luminous flux, luminous intensity, illuminance and Lambert radiator.

The luminous flux, expressed in lumen (*lm*), is defined as the quantitative expression of the brilliance of a source of visible light, and can be written as

$$\Phi = K_m \int_{400}^{780} V(\lambda)\Phi_e(\lambda)d\lambda \tag{2.7}$$

where K_m is the relationship between the physical radiometric unit watt and the physiological photometric unit lumen. (λ) is the spectral sensitivity of the human visual system proposed by the *Commission Internationale de l'Eclairage* in 1924 and finally, Φ_e is the radiant power or radiant flux expressed in watts (W). The integral interval from equation (2.7) varies between [400-780] nm since it corresponds to the visible spectrum wavelength band where the LED is functioning. Luminous intensity is defined as the luminous flux per unit solid angle at a certain direction, expressing the brightness of an LED in candela (cd) and is given as

$$I = \frac{d\Phi}{d\Omega} \tag{2.8}$$

where, Φ is the luminous flux and Ω the spatial angle.
Illuminance is the measurement of the amount of light falling onto (illuminating) and spreading over a given surfaced. It is represented as the luminous flux received in a unit area expressed in lux (lx) and can be written as

$$\boldsymbol{E = \frac{d\Phi}{dS}} \tag{2.9}$$

in which $\boldsymbol{dS}$ is the area of lighting and $\boldsymbol{d\Phi}$ the luminous flux received from $\boldsymbol{dS}$. In general, considering an LED as the transmission source, the maximum illuminance is positioned in the middle of the LED thus leading to a maximum output power. A Lambert radiator, depicted in figure 2-10, is a radiation model where the luminance is constant in all directions, albeit with different luminous intensity levels. In a VLC system, an LED used as a light source can be approximated to a lambert radiator, hence the luminous intensity distribution function can be expressed as

$$\boldsymbol{I}(\Phi) = \boldsymbol{I}(\mathbf{0})(\boldsymbol{cos}^{\boldsymbol{m_l}}(\Phi) \tag{2.10}$$

where $\boldsymbol{I}(\mathbf{0})$ is the center of luminous intensity and $\boldsymbol{m_l}$ is the order of Lambertian emission expressing the directivity of the source beam, given by [**Ped18**]

$$\boldsymbol{m_l = -\frac{ln(2)}{ln(cos\,\Phi_{\frac{1}{2}})}} \tag{2.11}$$

where $\Phi_{\frac{1}{2}}$ stand as the transmitter semi-angle at half power.

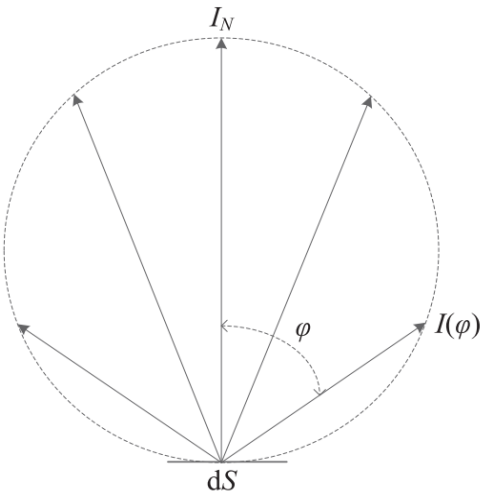

Figure 2-10: Representation of a Lambert radiator

2.3.2. Channel Modelling:

VLC system uses a technique where the links are based on IM/DD, figure 2-11, principally due to its reduced cost and complexity. On the transmitter side, intensity modulation is employed by the modulating signal $\boldsymbol{m(t)}$ varying the drive current of the LED, which in turn varies the intensity of the optical source $\boldsymbol{x(t)}$. On the receiver side, direct-detection is performed by a photodetector that generates a photocurrent $\boldsymbol{y(t)}$, directly proportional to the incident instantaneous optical power.

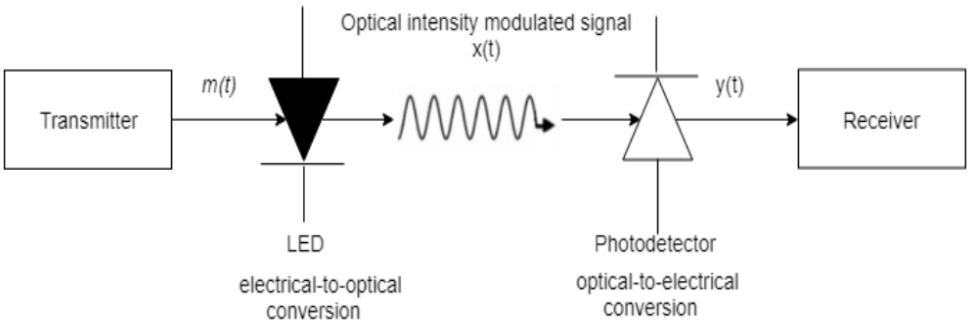

Figure 2-11: Block diagram of Intensity Modulation/Direct-Detection method.

As $\boldsymbol{x(t)}$ represents the optical power, this imposes two constraints on the transmitted signal. The first one reveals that $\boldsymbol{x(t)}$ must be nonnegative

$$\boldsymbol{x(t) \geq 0} \tag{2.12}$$

Lastly, the average value of $\boldsymbol{x(t)}$ must not exceed a maximum power value $\boldsymbol{P_{max}}$, as a result of eye safety requirements

$$\boldsymbol{P_{max} = \lim_{T\to\infty} \frac{1}{2T} \int_{-T}^{T} x(t)dt} \tag{2.13}$$

The transmitted power $\boldsymbol{P_t}$ indicates the transmitted power radiated from an LED. Considering $\boldsymbol{P_t}$ as in equation (2.13), the received power in a line-of-sight IM/DD link is given by

$$\boldsymbol{P_r = h(0)P_t} \tag{2.14}$$

where $\boldsymbol{h(0)}$ is the channel DC gain. The photocurrent at the receiver may be expressed as

$$\boldsymbol{y(t) = x(t) \otimes Rh(t) + n(t)} \tag{2.15}$$

$\boldsymbol{n(t)}$ is the additive white Gaussian noise (AWGN) and $\boldsymbol{h(t)}$ the impulse response of the channel, which is used to analyse and combat the effects of channel distortions. This channel distortion in VLC links manifests itself as the ISI. Considering an indoor line of sight (LOS) optical system propagation path as illustrated in figure 2-12, the transmitter is usually an LED fixed on the ceiling of the room directed downwards perpendicular to the floor, while the receiver, usually a photodetector, is pointing upward towards the direction of the transmitter.

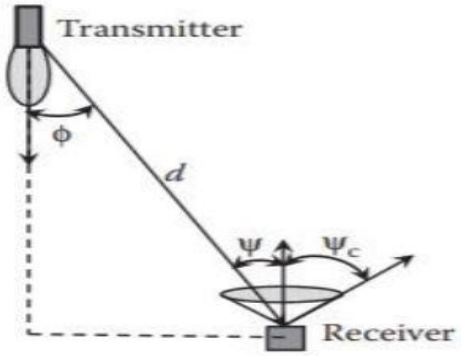

Figure 2-12: Transmitter and receiver geometry in a VLC system.

The angular distribution of the radiation intensity pattern modelled by a generalized Lambertian radiant intensity is given by

$$\boldsymbol{R_0(\phi)} = \begin{cases} \dfrac{(\boldsymbol{m_l}+\boldsymbol{1})}{\boldsymbol{2\pi}}\boldsymbol{cos^{m_l}(\phi)}, & \boldsymbol{\phi} \in \left[-\dfrac{\boldsymbol{\pi}}{\boldsymbol{2}}, \dfrac{\boldsymbol{\pi}}{\boldsymbol{2}}\right] \\ \boldsymbol{0}, & \boldsymbol{\phi} \geq \dfrac{\boldsymbol{\pi}}{\boldsymbol{2}} \end{cases} \tag{2.16}$$

where $\boldsymbol{\phi}$ is the angle with respect to transmitter or the irradiance angle. Taking into account $\boldsymbol{P_t}$ as the transmitted power, the radiant intensity is expressed as follows

$$\boldsymbol{S(\phi)} = \boldsymbol{P_t}\frac{(\boldsymbol{m_l}+\boldsymbol{1})}{\boldsymbol{2\pi}}\boldsymbol{cos^{m_l}(\phi)} \tag{2.17}$$

On the receiver side, the photodetector is modelled as an active area $\boldsymbol{A_r}$. Only radiation incident at angles $\boldsymbol{\Psi}$ smaller than the receiver field of view (FOV) are collected by the photodetector. As a result, the effective collection area $\boldsymbol{A_{eff}}$ is given by

$$\boldsymbol{A_{eff}(\Psi)} = \begin{cases} \boldsymbol{cos\,\Psi}, & \boldsymbol{0 \leq \Psi \leq \dfrac{\pi}{2}} \\ \boldsymbol{0}, & \boldsymbol{\Psi > \dfrac{\pi}{2}} \end{cases} \tag{2.18}$$

where, $\boldsymbol{\Psi}$ is the angle of incidence on the photodetector. Ideally a large-area detector would be the most appropriate for an indoor VLC, in order to collect as much power as possible. However, manufacturing cost, junction capacitance and receiver noise all increase as the detector area gets larger. Also, receiver bandwidth decreases. From the constant radiance theorem, a transmitter and a receiver are considered in FOV when

$$\boldsymbol{A_{eff}\, sin\frac{\Psi_c}{2} \leq A_r} \tag{2.19}$$

The channel gain considering LOS from the transmitter (LED) to the receiver photodetector is given as follows

$$\boldsymbol{h(0) = \begin{cases} \frac{A_r(m_l+1)}{2\pi d^2} cos^{m_l}(\phi) g(\Psi) cos(\Psi), & 0 \leq \Psi \leq \Psi_c \\ 0, & elsewhere \end{cases}} \tag{2.20}$$

considering $\boldsymbol{d}$ as the distance between transmitter and receiver, $\boldsymbol{\Psi_c}$ the FOV semi angle of the receiver and $\boldsymbol{g(\Psi)}$ the optical concentrator gain expressed as

$$\boldsymbol{g(\Psi) = \begin{cases} \frac{n^2}{sin^2 \Psi_c}, & 0 \leq \Psi \leq \Psi_c \\ 0, & 0 \geq \Psi_c \end{cases}} \tag{2.21}$$

where $\boldsymbol{n}$ is the concentrator refractive index.
The electrical $\boldsymbol{SNR}$ for an indoor VLC system, can be expressed in terms of the photodetector responsivity, received optical power and the total noise variance $\boldsymbol{\sigma^2}$, as

$$\boldsymbol{SNR = \frac{(RP_r)^2}{\sigma^2}} \tag{2.22}$$

where $\boldsymbol{\sigma^2}$ is equal to

$$\boldsymbol{\sigma^2 = {\sigma_{shot}}^2 + {\sigma_{thermal}}^2} \tag{2.23}$$

Analysing the total noise variance equation, $\boldsymbol{{\sigma_{shot}}^2}$ represents the variance caused by shot-noise in the detector that results from the received signal and is given by

$$\boldsymbol{{\sigma_{shot}}^2 = 2qRP_rB = 2qRP_{bg}I_2B} \tag{2.24}$$

where $\boldsymbol{B}$ is the bandwidth of the electrical filter that follows the photodetector, $\boldsymbol{P_{bg}}$ the background radiated power and $\boldsymbol{I_2}$ is the noise bandwidth factor that accounts for a rectangular transmitter pulse shape with a value of 0.562.
The potential interference introduced by optical noise originated from natural light or fluorescent light sources, act as unmodulated sources at the receiver and increases shot noise. One way to reduce the impact of this type of interference is to transmit in a narrow FOV which leads to a low optical noise alongside a higher optical signal gain. The variance in the detector caused by thermal noise, $\boldsymbol{\sigma_{thermal}}^2$ is expressed as

$$\boldsymbol{\sigma_{thermal}}^2 = \frac{\boldsymbol{8\pi K T_A}}{\boldsymbol{G}} \boldsymbol{C_{pd} A_r I_2 B^2} + \frac{\boldsymbol{16\pi^2 K T_A \Gamma}}{\boldsymbol{g_m}} \boldsymbol{C_{pd}}^2 \boldsymbol{A_r}^2 \boldsymbol{I_3 B^3} \tag{2.25}$$

where $\boldsymbol{T_A}$ is the absolute temperature of the environment, $\boldsymbol{G}$ is the open-loop voltage gain, $\boldsymbol{C_{pd}}$ is the fixed capacitance of photodetector per unit area, $\boldsymbol{\Gamma}$ is the field-effect transistor (FET) channel noise factor, $\boldsymbol{g_m}$ is the FET transconductance and $\boldsymbol{I_3}$ is the noise bandwidth factor that accounts for a full raised-cosine equalized pulse shape with a value of 0.0868. [**Ped18**].

2.3.2.1. Optical-OFDM Transmission System (O-OFDM):

In order to efficiently transmit information, the available channel bandwidth must be used effectively, taking into account transmitter power constraints and receiver complexity constraints. To define a channel characteristic, time dispersion is an essential parameter. It reflects a signal distortion manifested by the distribution of the modulation symbols, also known as delay spread, in the time domain. The phenomenon of the ISI illustrates this. Additionally, since the coherence bandwidth is inversely proportional to the delay spread, it can also be reflected in the frequency domain. As a result, a high delay spread results in a lower coherence bandwidth translating into a higher channel frequency selectivity (fading).
The information sequence is transmitted serially (symbol by symbol) at a particular speed in an SCM scheme. Since modern telecommunications systems need high data rates for transmission, these types of modulation systems suffer from ISI problems. The symbol length $\boldsymbol{T_s}$ will be very small due to high data rates. Therefore, the delay spread is greater than the length of the introductory ISI symbol, resulting in a reduction in the SNR obtained. The delay spreads are compensated by the use of equalization techniques, but their random characteristics make them difficult to predict, as a consequence of the complex and costly use of equalizers in an SCM scheme with delay spread. The implementation of MCM, which consists of splitting the high data rate channel over a number of subcarriers with a lower data rate, is one way to address the ISI problem of SCM, resulting in a greater symbol length in the subcarrier. The delay spread is therefore much smaller than the length of the symbol. In these terms there is no dispersion, turning the channel to a flat fading channel that can be easily estimated and compensated using a single equalization.
The principle is simple: the information sequence is transmitted parallelly, at adjacent frequencies, as a summation of a number of subcarriers. Mathematically, the available

channel bandwidth $\boldsymbol{W}$, is divided in $\boldsymbol{N_{sc}}$ subcarriers of relatively narrow width $\boldsymbol{\Delta f = W/N_{sc}}$. If Δf is sufficiently small, the channel frequency response ($\boldsymbol{f}$) is constant across each subcarrier, thus ISI is negligible.

Theoretically, as the number of subcarriers grows, better efficiency can be obtained as greater delay spreads can be treated. However, if, as the number of subcarriers increases, the available bandwidth remains similar, subcarrier frequencies are allocated similar to each other. Therefore, to decrease the frequency mismatch, the receiver synchronization components must be very specific. This makes the components of receivers expensive and complex. A fair trade-off between the spacing of the subcarriers and the number of subcarriers must therefore be achieved.

The OFDM, which is a modulation and multiplexing system where the channel bandwidth is split into overlapping subcarriers with a lower data rate, resulting in higher spectral efficiency, is a widely used type of MCM. OFDM symbols without ICI are created by the fact that the overlapping subcarriers are orthogonal to each other. In an OFDM system, the symbol rate $\boldsymbol{1/T}$ is reduced by a factor of $\boldsymbol{N_{sc}}$ subcarriers comparing to the symbol rate of a single carrier transmission scheme. Consequently, the symbol interval is $\boldsymbol{T = N_{sc}T_s}$, where $\boldsymbol{T_s}$ is the symbol interval in a single-carrier system. As mentioned before, if $\boldsymbol{N_{sc}}$ is sufficiently large, the symbol interval in an OFDM system can be made significantly larger than the time duration of the channel dispersion, hence ISI is almost negligible. A basic VLC-OFDM transmission system scheme is shown in figure 2-13.

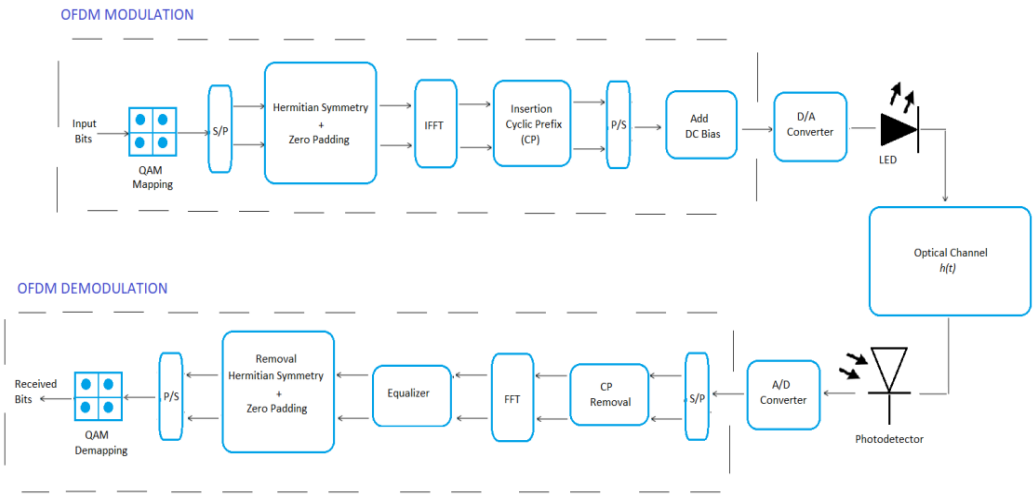

Figure 2-13: Block diagram of an O-OFDM transmission system.

A group of input bits are mapped to corresponding constellation points, usually QAM constellations, in the block diagram model of an O-OFDM transmission scheme, as shown above, first taking the OFDM modulation side. A serial to parallel converter is then implemented and the symbols are collected in parallel streams. Hermitian Symmetry (HS), a Discrete Fourier Transform (DFT) property, and zero padding are used. The first is used to obtain a real-value time-domain signal, removing the complex part of an OFDM signal since it cannot be transmitted through a single LED signal. The latter allows having a power-of-two length OFDM signal, speeding up the processing time as well as improving the efficiency of fast Fourier transform (FFT) algorithms. Furthermore, an inverse FFT (IFFT) algorithm is

performed to compute the inverse DFT (IDFT), converting the symbols from frequency to discrete time domain besides modulating the mapped symbols into subcarriers of an OFDM symbol. Then the CP, consisting of a cyclic extension from the end of the OFDM signal, is applied to the beginning of the OFDM symbol, preserving orthogonality among the subcarriers, thus reducing the ICI. As well as serving as a guard gap and thereby removing ISI. As a combination of all IFFT subcarriers, the data is multiplexed. In the time-domain IFFT, the output is a bipolar signal at this point. The OFDM signal must, however, be unipolar in order to be transmitted by an LED, as the light intensity cannot be negative. This implies that between zero volts and any arbitrary positive voltage, the signal values are constrained to be. Otherwise, due to under-driving the LED can be impaired or it could not be illuminated. In general, to obtain non-negative signals, there are different optical OFDM approaches. Asymmetrically clipped optical OFDM (ACO-OFDM) is one of these approaches, whereas direct current (DC)-biased optical OFDM (DCO-OFDM) is the other approach.

A digital-to - analog converter (DAC) is then used to convert the digital time-domain data to analog time-domain data. To transmit the OFDM signal through an optical wireless channel an LED is used, that causes signal distortions and time dispersion. A photodetector which converts the optical source to a proportional electric current will then detect the signal. Then an Analog-to-Digital Converter (ADC) samples the signal at a frequency of $\boldsymbol{1/T}$, transforming the analog waveform into a digital signal. The ADC output should be equal to the DAC input for an ideal channel. As the conversion from analog to digital takes place, the synchronization of the receiver is realized by a correlation between the signal received and transmitted. These methods of synchronization will not, however, be examined. Once the OFDM signal is divided by the OFDM demodulation side into parallel carriers, the CP extension of each OFDM symbol is eliminated.

FFT algorithm is executed to demodulate the OFDM subcarriers into QAM symbols. An equalizer is then used to compensate for channel distortions, consisting of the addition of training symbols to approximate the characteristics of the channel. The one-tap equalizer can be achieved by an OFDM scheme, meaning the equalizer transfer function must be equal to the inverse of the channel transfer function. The parallel subcarriers are finally compiled into a single stream in which the mapped symbols are demapped and the symbols are translated back to the original input bits. [**Ped18**]

2.3.2.1.1. Direct-Current (DC) biased O-OFDM (DCO-OFDM):

DCO-OFDM is one of the most studied modulation methods proposed by Carruthers and Kahn for VLC. As shown in the figure 2-14, consider a DCO-OFDM transmission with $\boldsymbol{N}$ subcarriers.

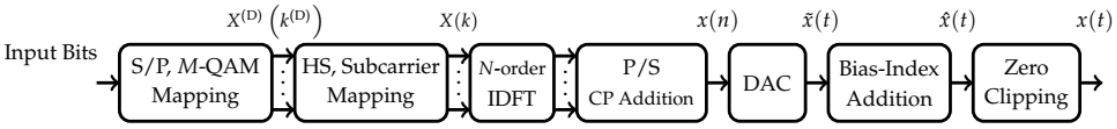

Figure 2-14: Block diagram of DCO-OFDM Transmitter.

The serially incoming bits are parsed into $\boldsymbol{N/2 - 1}$ parallel streams. These bits are modulated to Gray-mapped complex *M*-ary quadrature-amplitude modulation (QAM) alphabets drawn from the constellation set $\boldsymbol{Q = \{Q_0, Q_1, \ldots\ldots\ldots, Q_{M-1}\}}$, resulting in FD symbols, $\boldsymbol{X^{(D)}(k^{(D)})}$, $\boldsymbol{K^{(D)} = 0, 1, \ldots\ldots N/2 - 1}$, The $\boldsymbol{N/2 - 1}$ FD symbols are assigned to a *N*-dimensional signal, $\boldsymbol{X(k)}$, $\boldsymbol{k = 0, 1, \ldots\ldots N - 1}$ obeying HS

$$\boldsymbol{X(k) = \begin{cases} X^{(D)}\left(k^{(D)}\right), & k = k^{(D)} + 1 \\ X^{*(D)}\left(k^{(D)}\right), & k = N - (k^{(D)} + 1) \\ 0, & elsewhere \end{cases}} \tag{2.26}$$

where$(.)^*$ represents the conjugate operation. To avoid any residual complex component in the TD signal, $\boldsymbol{X(0)}$, and $\boldsymbol{X(N/2)}$, are set to zero. Note that, HS is incorporated to obtain a real-valued TD signal. A graphical illustration of the real and the imaginary components of $\boldsymbol{X(k)}$, i.e, $\boldsymbol{\Re[X(k)]}$ and $\boldsymbol{\Im[X(k)]}$, is presented in Figure 2-15(a) and Figure 2-15(b), respectively to signify the impact of HS on the generation of TD signal. It can be observed from Figure 2-15(a) that the real components of the second half of subcarriers are the mirrored image of the first half of the subcarriers. Moreover, from Figure 2-15(b), it may be noticed that the imaginary components of the second half of $\boldsymbol{X(k)}$, are inverted mirror image of the imaginary components of the first half.

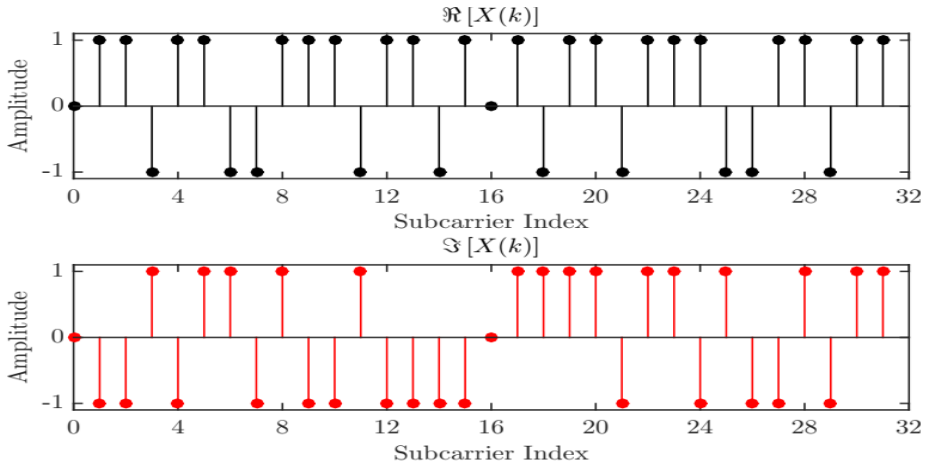

Figure 2-15: HS illustration for 4-QAM DCO-OFDM. (a) $\boldsymbol{\Re[X(k)]}$ and $\boldsymbol{\Im[X(k)]}$.

The Hermitian symmetric FD symbols, $\boldsymbol{X(k)}$, are fed to *N*-order IDFT to multiplex the orthogonal subcarriers which results a TD signal given by

$$\boldsymbol{x(n) = IDFT[X(k)]} \tag{2.27}$$

for $\boldsymbol{n = 0, 1, \ldots, N - 1}$. It is highlighted that due to HS, $\boldsymbol{x(n)}$ is real-valued but bipolar. An example of the conversion of complex FD symbol incorporating HS to real-valued TD signal

is illustrated in Figure 2-16. It is demonstrated that if HS is enforced in the FD, the output TD signal would be real-valued

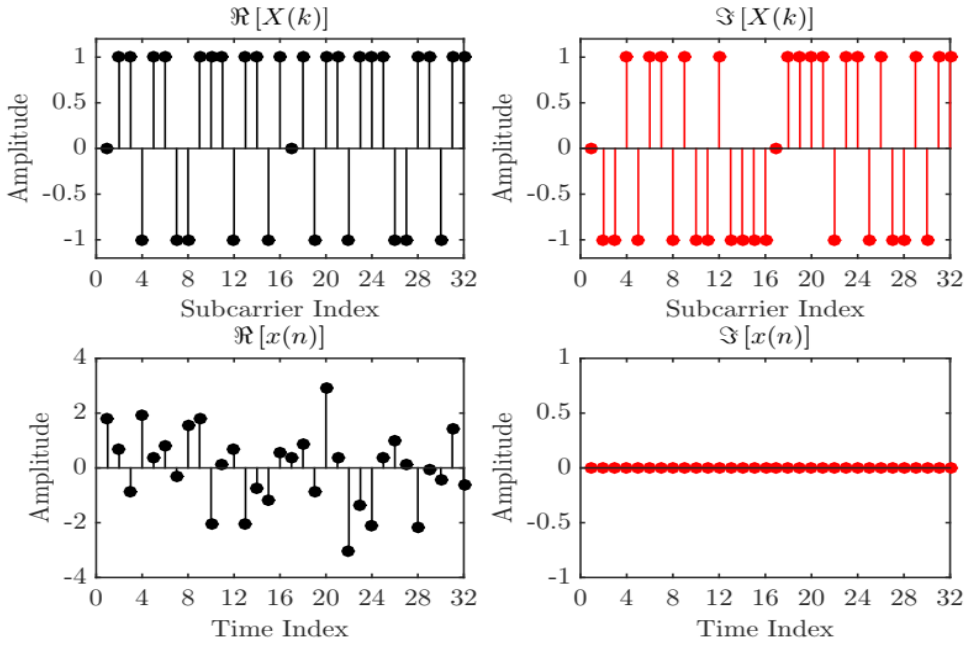

Figure 2-16: An example of DCO-OFDM signal conversion from FD to TD with HS.

A continuous TD signal $\tilde{\boldsymbol{x}}(\boldsymbol{t})$ is obtained by feeding $\boldsymbol{x}(\boldsymbol{n})$ to a DAC and adding a cyclic prefix (CP) of length $\boldsymbol{N_{CP}}$ which is, at least equal to the root-mean-square (rms) delay spread of the channel. In order to convert the bipolar signal into a unipolar signal, a forthright approach is to add suitable bias-index, $\boldsymbol{\beta_{DC}^{(D)}}$. $\boldsymbol{\beta_{DC}^{(D)}}$ is prescribed relative to the standard deviation of $\tilde{\boldsymbol{x}}(\boldsymbol{t})$ as:

$$\boldsymbol{\beta_{DC}^{(D)} = \varsigma_{(D)}\sqrt{E(|\tilde{x}(t)|^2)}, \quad \varsigma_{(D)>0}} \tag{2.28}$$

where $\boldsymbol{\varsigma_{(D)}}$is the constant of proportionality. The bias-index on the decibel (dB) scale is defined as $\boldsymbol{10\,log_{10}(\varsigma^2{}_{(D)} + 1)}$ dB. The TD signal after the addition of $\boldsymbol{\beta_{DC}^{(D)}}$ is

$$\hat{\boldsymbol{x}}(\boldsymbol{t}) = \tilde{\boldsymbol{x}}(\boldsymbol{t}) + \boldsymbol{\beta_{DC}^{(D)}}. \tag{2.29}$$

Numerous levels of bias-index can be incorporated in the bipolar signal. The most convenient approach is to adopt *sufficient biasing*, in which, $\boldsymbol{\varsigma_{(D)}}$ is adjusted such that all the negative excursions of $\hat{\boldsymbol{x}}(\boldsymbol{t})$ after the addition of $\boldsymbol{\beta_{DC}^{(D)}}$ are eliminated. However, in these cases, the value of $\boldsymbol{\beta_{DC}^{(D)}}$ is relatively large, which renders DCO-OFDM inefficient in term of optical power. Hence, a better option can be to employ a moderate value of $\boldsymbol{\beta_{DC}^{(D)}}$ and eliminate the remaining negative peaks by hard clipping $\hat{\boldsymbol{x}}(\boldsymbol{t})$ as:

$$x(t) = \begin{cases} \hat{x}(t), & \hat{x}(t) \geq 0 \\ 0, & \hat{x}(t) < 0 \end{cases} = \hat{x}(t) + n_c(\beta_{DC}^{(D)}) \tag{2.30}$$

where $n_c(\beta_{DC}^{(D)})$ is $\beta_{DC}^{(D)}$ dependent clipping noise, which can severely impact the performance of the system. A graphical illustration of the biasing expressed in (2.29) and the clipping process after adding the bias-index given in (2.30) is given in Figure 2-17.

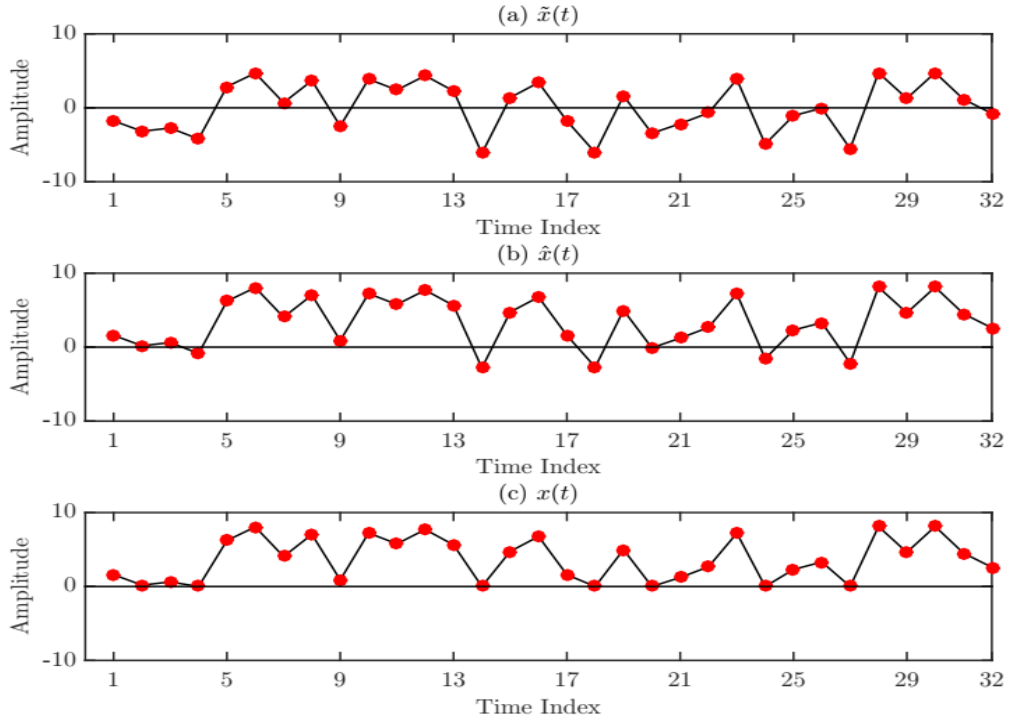

Figure 2-17: TD representation of DCO-OFDM (a) signal before biasing, $\tilde{x}(t)$ (b) biased signal, $\hat{x}(t)$ (c) biased signal after clipping, $x(t)$

$n_c(\beta_{DC}^{(D)})$ can be decreased by increasing $(\beta_{DC}^{(D)})$. For sufficient biasing $n_c(\beta_{DC}^{(D)}) = 0$. Moreover, with an increase in *N*, the PAPR increases. Therefore, larger values $(\beta_{DC}^{(D)})$ are required to minimize $n_c(\beta_{DC}^{(D)})$. On the other hand, if smaller $(\beta_{DC}^{(D)})$ is utilized, more subcarriers are affected by the clipping process. The impact of adding bias-index on DCO-OFDM constellation in a noise-less scenario (only the impact of clipping noise due to remaining negative excursions) is illustrated in Figure 2-18. It is observed that for lower bias-index, the recovered constellation (after clipping) has a larger splatter around the ideal constellation points due to exacerbated clipping noise. However, with an increase in value of bias index, the clipping noise decreases, therefore, the recovered constellation is almost identical to the ideal constellation.

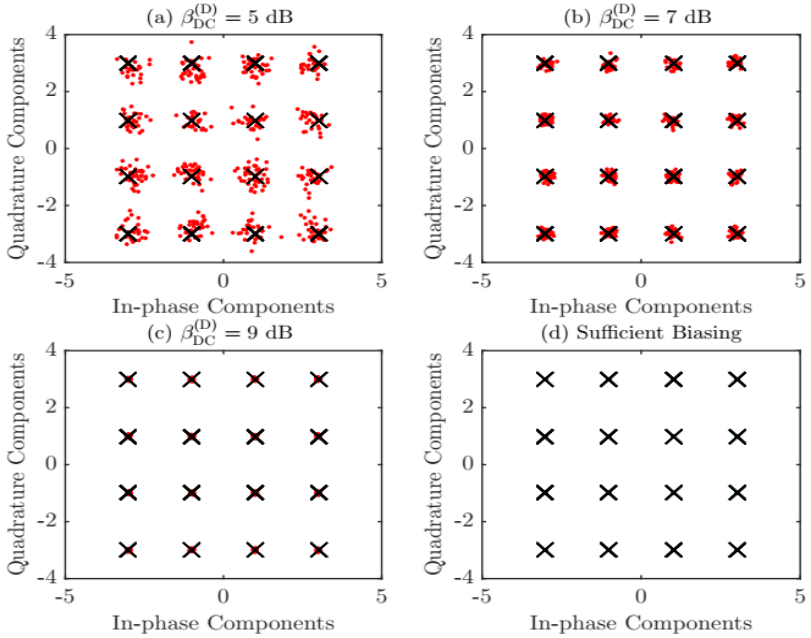

Figure 2-18: The impact of increasing bias, $(\beta_{DC}^{(D)})$ on the clipping noise, $(\beta_{DC}^{(D)})$ using M = 16‡.

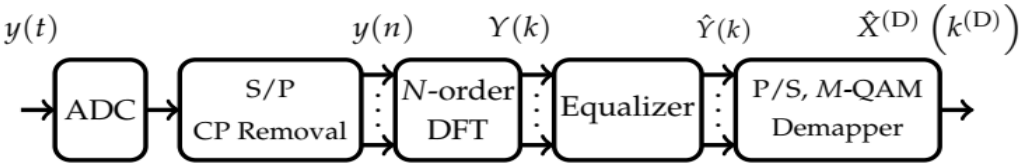

Figure 2-19: Block diagram of DCO-OFDM Receiver.

At the receiver Figure 2-19, $\boldsymbol{y(n)}$ is obtained by impinging the photo-detected signal $\boldsymbol{y(n)}$, on ADC followed by S/P conversion and CP removal. The received FD symbols, $\boldsymbol{Y(k)}$are obtained by *N*-order DFT as:

$$\boldsymbol{Y(k) = DFT[y(n)] = H(k)X(k) + W(k)} \tag{2.31}$$

where $\boldsymbol{H(k)}$ is the channel frequency response for the $\boldsymbol{k_{th}}$ subcarrier. Subsequently, a single-tap equalization is perfomed in the FD, which results in

$$\boldsymbol{\hat{Y}(k) = \hat{X}(k) + Z(k)} \tag{2.32}$$

where $\boldsymbol{\hat{X}(k)}$ are the estimated received FD symbols after (zero-forcing) equalization and $\boldsymbol{Z(K) = W(k)/H(k)}$.
The transmitted data is detected as:

$$\boldsymbol{\hat{X}^{(D)}\left(k^{(D)}\right) = arg \min_{X_Q \in Q} \left\| \hat{Y}\left(k^{(D)} + 1\right) - X_Q \right\|} \tag{2.33}$$

where $\boldsymbol{X_Q}$ represents all the elements in $\boldsymbol{Q}$.

To evaluate the SE (spectral efficiency), consider *M*-ary QAM alphabets and *N* subcarriers which are separated by the symbol duration $\boldsymbol{T_{sym}}$. Hence, the total bilateral bandwidth $\boldsymbol{B}$ is $\boldsymbol{N/T_{sym}}$. After the addition of CP, the O-OFDM symbol duration is given as $\boldsymbol{T_{OFDM} = T_{sym} + T_{CP}}$, where, $\boldsymbol{T_{CP}}$ is the CP duration. Since, in DCO-OFDM, only $\boldsymbol{N/2 - 1}$ subcarriers are modulated, therefore, the data rate $\boldsymbol{R_b}$ is $\boldsymbol{10\, log_2(M)(\, N/2\, - 1)/T_{OFDM}}$. Thus, the SE of DCO-OFDM $\boldsymbol{\eta_{DCO}}$ is given as:

$$\boldsymbol{\eta_{DCO} = \frac{R_b}{B} = \frac{log_2(M)(\, N/2\, - 1)}{N + N_{CP}}, \quad (bit/s/Hz)} \tag{2.34}$$

[Ali18]

2.3.2.1.2. Asymmetrically Clipped O-OFDM (ACO-OFDM):

ACOOFDM is another method that completely prevents the bias-index from realizing a non-negative TD signal. Since no bias-index is needed, however, ACO-OFDM is more energy efficient compared to DCO-OFDM, only for alphabets of lower order modulation. Armstrong and Lowery suggested this system. Transmission of ACO-OFDM with N subcarriers would be considered. The ACO-OFDM block diagram is shown in Figure 2-20

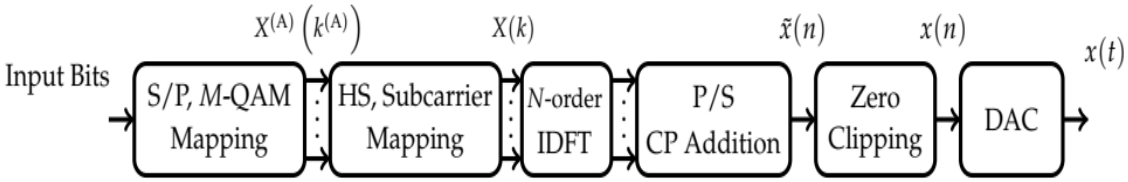

Figure 2-20: Block diagram of ACO-OFDM Transmitter.

The serially incoming bits streams are mapped onto *N*/4 *M*-ary QAM alphabet $\boldsymbol{X^{(A)}(k^{(A)})}$, $\boldsymbol{k^{(A)} = 0, 1, \ldots\ldots, N/4\, - 1}$. drawn from constellation set $\boldsymbol{Q}$ after serial-to-parallel conversion (S/P). The symbols, $\boldsymbol{X^{(A)}(k^{(A)})}$ are then assigned to odd indexes/subcarriers of *N*-dimensional signal $\boldsymbol{X(k)}$, $\boldsymbol{k = 0, 1, \ldots\ldots, N - 1}$ as:

$$\boldsymbol{X(k) = \begin{cases} X^{(A)}\left(k^{(A)}\right), & k = 2k^{(A)} + 1 \\ X^{*(A)}\left(k^{(A)}\right), & k = N - (2k^{(A)} + 1) \\ 0, & elsewhere \end{cases}} \tag{2.35}$$

and HS is also enforced. Via *N*-order IDFT, a TD signal, i.e.

$$\boldsymbol{\tilde{x}(n) = IDFT[X(k)]} \tag{2.36}$$

is obtained, where, $\boldsymbol{n = 0, 1, \ldots\ldots, N-1}$ The frame structure of $\boldsymbol{X(k)}$ ensures that $\tilde{\boldsymbol{x}}(\boldsymbol{n})$ is anti-symmetric, i.e.,

$$\tilde{\boldsymbol{x}}\left(\tilde{\boldsymbol{n}}^{(A)}\right) = -\tilde{\boldsymbol{x}}(\tilde{\boldsymbol{n}}^{(A)} + \frac{\boldsymbol{N}}{\boldsymbol{2}}) \tag{2.37}$$

for $\tilde{\boldsymbol{n}}^{(A)} = \boldsymbol{0, 1, \ldots\ldots, N/2-1}$. Because of this anti-symmetric property, the negative excursions of $\tilde{\boldsymbol{x}}(\boldsymbol{n})$ can be clipped to zero using hard clipping process without loss of useful information to yield:

$$\boldsymbol{x(n)} = \lfloor \tilde{\boldsymbol{x}}(\boldsymbol{n}) \rfloor = \begin{cases} \tilde{\boldsymbol{x}}(\boldsymbol{n}), & \tilde{\boldsymbol{x}}(\boldsymbol{t}) > \boldsymbol{0} \\ \boldsymbol{0}, & \tilde{\boldsymbol{x}}(\boldsymbol{t}) \leq \boldsymbol{0} \end{cases} \tag{2.38}$$

where $\lfloor . \rfloor$ represents the zero level clipping process. The zero level clipping process results in a unipolar signal which is compatible with IM-DD. A graphical illustration of $\tilde{\boldsymbol{x}}(\boldsymbol{n})$ and $\boldsymbol{x}(\boldsymbol{n})$ is portrayed in Figure 2-21, where it is illustrated that after zero level clipping process all the negative amplitudes of the TD ACO-OFDM signals are eliminated.

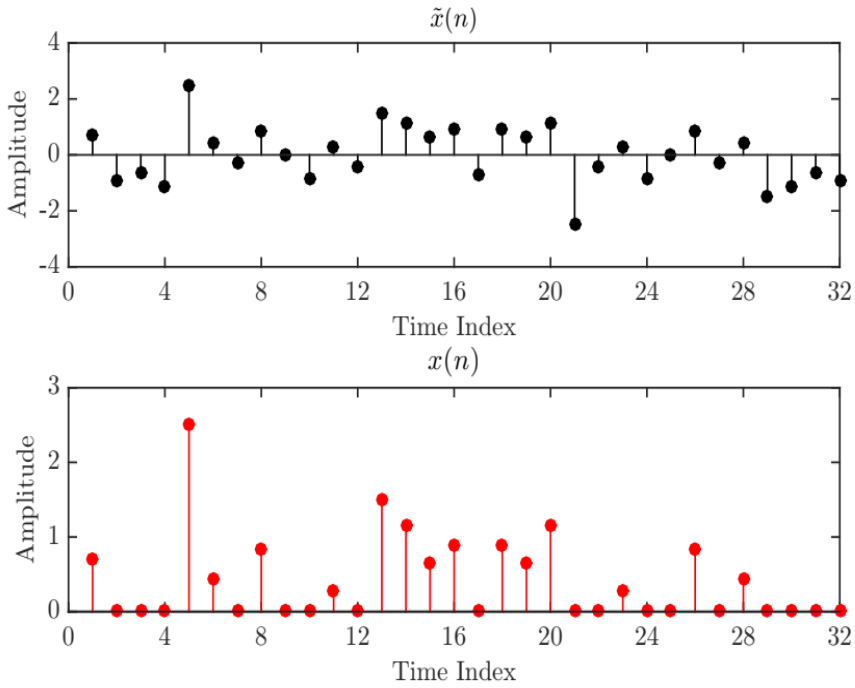

Figure 2-21: TD representation of ACO-OFDM signal before and after clipping.

In the FD, the clipping distortion, $\boldsymbol{N_c(k)}$ resulting from the zero level clipping in (2.38) only impacts the even subcarriers, while the odd subcarriers remain unaffected. So, the symbols can be readily extracted by choosing the data-carrying odd subcarriers. However, the amplitude of the symbols is reduced to half because of clipping operation. The mathematical representation of FD counterpart of $\boldsymbol{x(n)}$ is given as:

$$X_c(k) = \begin{cases} X(k)/2, & k = 2k^{(A)} + 1 \\ N_c(k), & k = N - (2k^{(A)} + 1) \end{cases} \tag{2.39}$$

The impact of clipping is graphically illustrated in Figure 2-22.

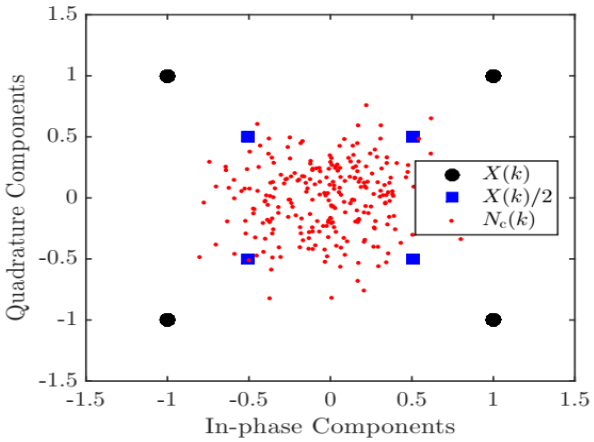

Figure 2-22: Constellation of ACO-OFDM before and after clipping (2.39) for 4-QAM. *Black* constellation points illustrate the data on odd subcarriers before clipping. *Blue* points after clipping. *Red* points depict the distortion on even subcarrier after clipping

After zero level clipping, $\boldsymbol{x(n)}$ is impinged on a DAC to obtain $\boldsymbol{x(t)}$ which is transmitted using LED to an optical wireless channel.

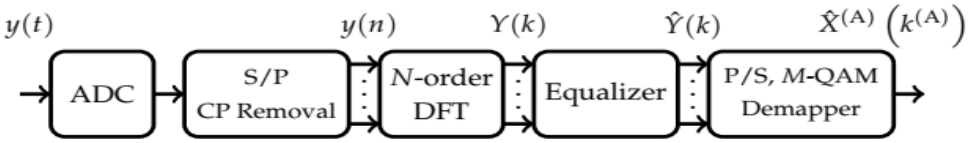

Figure 2-23: Block diagram of ACO-OFDM Receiver.

The receiver of ACO-OFDM is portrayed in Figure 2-23. $\boldsymbol{y(n)}$ is obtained after analog-to-digital conversion of $\boldsymbol{y(n)}$.Via *N*-order DFT, $\boldsymbol{y(n)}$ is transformed into a FD signal on which the equalization is performed. Subsequent to the equalization process, $\widehat{\boldsymbol{Y}}(\boldsymbol{k})$ is obtained (same as depicted in (2.32)), from which the transmitted symbols can be detected as:

$$\widehat{\boldsymbol{X}}^{(A)}\left(\boldsymbol{k}^{(A)}\right) = \boldsymbol{arg}\min_{\boldsymbol{X_Q} \in \boldsymbol{Q}} \left\| \widehat{2\boldsymbol{Y}}\left(2\boldsymbol{k}^{(DA)} + \boldsymbol{1}\right) - \boldsymbol{X_Q} \right\| \tag{2.40}$$

where the factor of 2 is to counterbalance the impact of halving of the amplitude of the symbols In ACO-OFDM, only *N*/4 among *N* available subcarriers can be modulated, since half of the subcarriers are sacrificed to satisfy HS, whereas, the remaining *N*/4 subcarriers are used to realize an anti-symmetric TD signal. Therefore, following the same approach as in DCO-OFDM, the SE of ACO-OFDM is evaluated as:

$$\eta_{ACO} = \frac{log_2(M)(N/4)}{N + N_{CP}}, \quad (\mathbf{bit/s/Hz}) \tag{2.41}$$

From (2.41) it is deduced that $\eta_{ACO} = 0.5\eta_{DCO}$ for same CP length. So, for the same constellation size, *M*, and sampling frequency, the data-rate of DCO-OFDM is twice as compared to ACO-OFDM. [**Ali18**]

2.3.3. VLC weak-points:

As exposed by now, VLC is a technology that has plenty of important advantages. However, like any other technology, VLC has also several drawbacks. Some of the disadvantages are due to the early stage of the VLC technology and could be overtaken as the technology is fully developed. The others ones are due to the usage of the light and its characteristics. For the later ones, it will be difficult to completely mitigate them, but their effects could be reduced or the communication could be adapted to the situations. The strongest disadvantages of VLC and the possible solutions for their mitigation will be further discussed.

- *Stringent LoS condition:* Generally, LoS maximizes the power efficiency and minimizes multipath distortion. In some of the cases the mandatory LoS condition can be considered as an advantage because the interferences from other receivers are limited and the communication security is enhanced. However, there are other applications where this issue is considered as a strong disadvantage. Non-LoS communications are considered to be more reliable, flexible and robust. The mandatory LoS condition has a negative effect on mobility and, in some areas, it represents VLC's greatest disadvantage because an object interposed between emitter and received can block the communication, unless an alternate route is available. *Possible solution:* By using multi-hop communications and retransmissions, the data can reach at users that are located outside the emitter's LoS but are in the LoS of another transceiver. An alternative solution for this problem is to combine VLC with RF. In this case, when a node cannot be addressed by VLC it is addressed by RF.
- *Limited transmission range:* When considering the transmission range, VLC cannot compete with RF communications. Even if the VLC transmission range can be increased by optimizing the emitter and receiver parameters, VLC communication range is still significantly shorter than RF communication range. On the emitter's side, the communication range can be increased by increasing the transmission power or by using a more directive light beam. On the receiver's side, the range can be increased by using different techniques for Signal to Noise Ratio (SNR) enhancement, such as narrow Field of View (FOV) receiver, optical lens or different filtering techniques *Possible solution:* Besides the enhancement of the emitter and receiver, the multi-hop networking can be again a solution that significantly increases the communication range of VLC systems.
- *Susceptibility to interferences:* Another disadvantage of the VLC is its susceptibility to interferences. VLC is likely to be affected by other illuminating devices such as incandescent or fluorescent light sources. Generally, these light sources produce low

frequency noise which can be removed with a high pass filter. Besides the artificial light sources, in outdoor applications, the sunlight represents a very strong perturbing factor. The sun produces unmodulated light which introduces a strong DC component that can be removed with capacitive DC filters. However, high intensity optical noise can saturate the receiver, blocking the communication. *Possible solution:* The effect of other light sources can be reduced by using optical filters, by reducing the receiver FOV and by filtering the unwanted frequencies. Even if the mentioned technique mitigates the effect of the interferences, high levels of noise still affect the communication performances.

2.4. Conclusion:

Visible light communication (VLC) is currently enjoying a promising development in the research area of communication. VLC transmits information with the visible light emitted by the light emitting diodes (LEDs), which are generally deployed to provide indoor illumination simultaneously. It can be complementary technology to the prevailing RF systems and can fulfill the requirements of Internet Of Thinks (IoT). In VLC, simple low-cost intensity modulation and direct detection (IM/DD) techniques are employed to send information, which implies that the phase cannot be used to convey any information.

In order to combat the inter-symbol interference caused by the indoor optical wireless channel, orthogonal frequency-division multiplexing (OFDM) has been considered for VLC due to its inherent robustness to multipath effect. In VLC, the transmitted electrical signal is used to modulate the light intensity of the LED. For this purpose, the transmitted electrical signal must be real and non-negative. Therefore, the traditional OFDM needs to be modified to obtain the real-valued signal.

VLC technologies can be used for various applications in homes, vehicles, aerospace, trains etc. without the constraint of limited usable spectral bandwidth.

CHAPTER 3:

PEAK TO AVERAGE POWER RATIO REDUCTION TECHNIQUES

3.1. Introduction:

As designers begin turning to OFDM system in system architectures, they will quickly realize that implementing this modulation scheme is not an easy task. Specifically, engineers are quickly learning that while ODFM provides some nice advantages to a wireless architecture, it also comes equipped with some design and implementation headaches.

OFDM is highly sensitive to time and frequency synchronization errors, and especially at frequency synchronization errors, everything can go wrong. Indeed, demodulation of an OFDM signal with an offset in the frequency can lead to a high bit error rate. The frequency synchronization errors occur by two factors: first one the difference between local oscillator frequencies in transmitter and receiver, and the second being relative motion between the transmitter and receiver that gives Doppler spread and resulting ICI. Other downside can face OFDM system is the multipath fading which can break the orthogonality. The Multipath propagation means the signal reaching the receiver by two or more paths ,subsequently it causes the multipath interference including constructive and destructive.

The major drawback of OFDM based system is high value of peak-to-average power ratio, this chapter provides a profound literature review on the PAPR of O-OFDM system, the detailed analysis of PAPR, its impact and definition and different methods of PAPR reduction are included.

SLM PAPR reduction technique is a potential candidate to give good results on mitigating PAPR problem, so we will study the concepts of this technique as well as examining its performance on a simulation program.

3.2. Peak-to-Average Power Ratio (PAPR):

The transmit signals in an O-OFDM system can have high peak values in the time domain since many subcarrier components are added via an IFFT operation. Therefore, O-OFDM systems are known to have a high PAPR, compared with single-carrier systems. In fact, the high PAPR is one of the most detrimental aspects in the O-OFDM system

3.2.1. Impact of PAPR on the system:

The O-OFDM system has intermittent peaks that occur throughout the length of the O-OFDM signal contributing immensely to the Peak-to-Average Power Ratio (PAPR). With non-constant amplitude signals, it is important to improve the PAPR of those signals. The presence of these high peaks means that the optical source will have to operate outside its linear region to accommodate the full amplitude signal swings. This is very undesirable as it increases the level of distortion present in the transmitted signal.

PAPR also decreases the SQNR (Signal-to-Quantization Noise Ratio) of ADC and DAC. DAC should have sufficient dynamic range to accommodate the large peaks of the OFDM signals because of the high PAPR. Even if, a high precision DAC supports high PAPR with low quantization noise but it is very expensive. In the other hand, low precision DAC is cheaper and its quantization noise is more. For large number of OFDM sub-carriers, O-OFDM signals follow the Gaussian distribution. In such type of distribution average of the

peak signal rarely occur and uniform quantization by the Analog to Digital Converter (ADC) is not desirable. [**Ain14**]

If clipping of the signal is done, in-band distortion and out-of-band expansion (adjacent channel interference) will be occurred. So, the major impacts of a high PAPR are:

- Reduction in efficiency the optical source.
- Increased complexity in the ADC and DAC.

3.2.2. Definition of PAPR:

The discrete form of OFDM signal $\boldsymbol{x(n)}$ is given by

$$\boldsymbol{x(n) = \frac{1}{\sqrt{N}} \sum_{k=0}^{N-1} X_k e^{\frac{j2\pi kn}{N}}, for\ n = 0, 1, 2, 3, \ldots . N-1} \tag{3.1}$$

The PAPR of the continuous time baseband OFDM transmitted signal $\boldsymbol{x(t)}$ is the ratio of the maximum instantaneous power and the average power.

By definition

$$\boldsymbol{PAPR = \frac{max[x(t)]^2}{E\{|x(t)|^2\}}, for\ 0 \leq t \leq NT} \tag{3.2}$$

where, $\boldsymbol{E}[.]$denotes expectation operator and $\boldsymbol{E\{[x(t)]^2\}}$is average power of $\boldsymbol{x(t)}$ as well as $\boldsymbol{T}$ is an original symbol period. [**Ain14**]

3.2.3. PAPR and Oversampling:

the PAPR for the discrete-time baseband signal $\boldsymbol{x(n)}$ may not be the same as that for the continuous-time baseband signal $\boldsymbol{x(t)}$. In fact, the PAPR for $\boldsymbol{x(n)}$ is lower than that for $\boldsymbol{x(t)}$, simply because $\boldsymbol{x(n)}$ may not have all the peaks of $\boldsymbol{x(t)}$. In practice, the PAPR for the continuous-time baseband signal can be measured only after implementing the actual hardware, including DAC. In other words, measurement of the PAPR for the continuous-time baseband signal is not straightforward. Therefore, there must be some means of estimating the PAPR from the discrete-time signal $\boldsymbol{x(n)}$. Fortunately, it is known that $\boldsymbol{x(n)}$ can show almost the same PAPR as $\boldsymbol{x(t)}$ if it is L-times interpolated (oversampled) where $L \geq 4$.

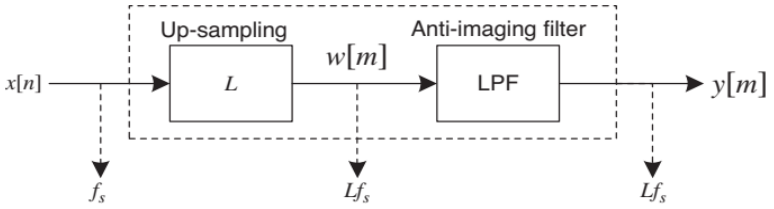

Figure 3-1: Block diagram of L-times interpolator.

Figure 3-1 shows the block diagram of interpolator with a factor of L. It inserts $(\boldsymbol{L-1})$ zeros between the samples of $\boldsymbol{x(n)}$ to yield $\boldsymbol{w(m)}$.

A low pass filter (LPF) is used to construct the L-times-interpolated version of $\boldsymbol{x(n)}$ from $\boldsymbol{w(m)}$. For the LPF with an impulse response of $\boldsymbol{h(m)}$, $\boldsymbol{y(m)}$ is the L-times-interpolated output signal.

Figures 3-2 and 3-3 illustrate the signals and their spectra appearing in the oversampling process with a sampling frequency of 2 kHz to yield a result of interpolation with L=4. [**Yon10**].

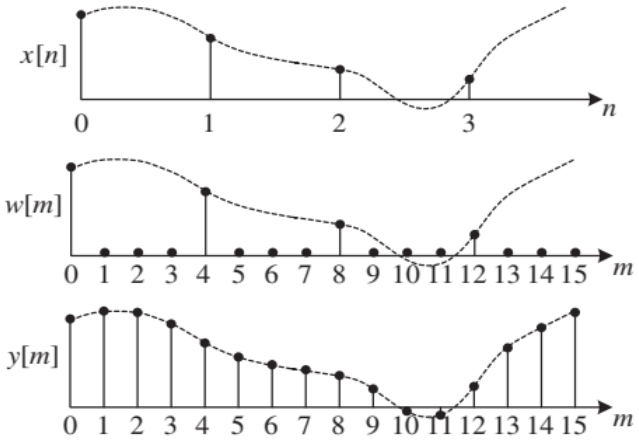

Figure 3-2: Interpolation with L =4 in the time domain.

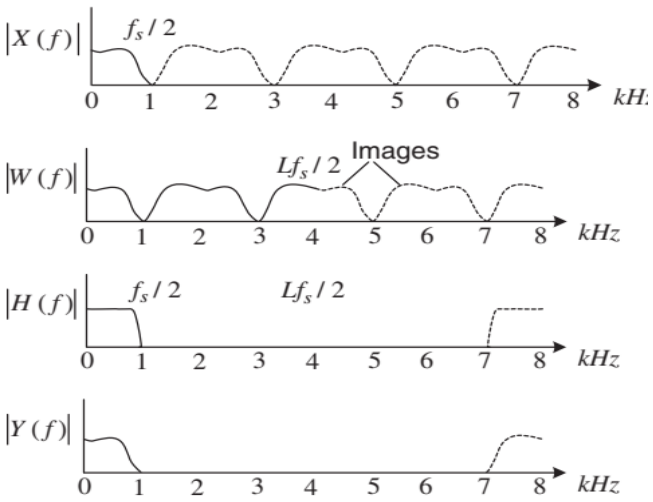

Figure 3-3: Interpolation with L =4 in the frequency domain.

3.2.4. Distribution of PAPR:

To design and develop an effective PAPR reduction technique, it is very important to accurately identify the distribution of PAPR in OFDM systems. The distribution of PAPR plays an important role in the design of the whole OFDM system. The distribution of PAPR can be used in determining the proper output back-off of the LED to minimize the total

degradation. It can be used directly to calculate the BER and to estimate the achievable information rates.

The power of OFDM signal has chi-square distribution. The distribution of PAPR is often expressed on the one hand Complementary Cumulative Distribution Function (CCDF). In probability theory and statistics, the CCDF describes the probability that a real-valued random variable X with a given probability distribution will be found at a value greater than or equal to x [**Jos12**].

The Cumulative Distribution Function (CDF) of the PAPR of the amplitude of a signal sample is given by

$$\boldsymbol{F(z) = 1 - exp(z)} \tag{3.3}$$

The CCDF of the PAPR of the data block desired in our case is to compare outputs of different reduction techniques.

This is given by:

$$\begin{aligned} \boldsymbol{Pr(PAPR > z)} &= \boldsymbol{1 - Pr(PAPR \leq \Upsilon)} \\ &= \boldsymbol{1 - F(z)^N} \\ &= \boldsymbol{1 - (1 - ex\,p(-\Upsilon))^N} \end{aligned} \tag{3.4}$$

Where, Υ is the given reference level.

$\boldsymbol{N}$ is the number of subcarriers

3.2.5. PAPR reduction techniques:

3.2.5.1. Review of PAPR reduction techniques:

PAPR reduction techniques for O-OFDM have been investigated in the literature were taxonomy of which is given in Figures 3-4 and are classified as

- *Signal Distortion Techniques*: In these techniques, high PAPR is reduced by distorting the O-OFDM signal prior to its transmission through the LED. Most common signal distortion techniques are (i) clipping and filtering, (ii) companding and (iii) peak windowing. The idea behind clipping of the signal is that the high peaks occur only rarely, therefore, small amount of distortions resulting from clipping the peaks can be tolerable. In companding, large amplitudes of the signal are compressed at the transmitter before being expanded at the receiver to recover the original waveform, but leading to significant increase of noise contribution.
- *Coding techniques*: In these techniques, coding schemes that are generally used for error detection and correction are adapted to perform the additional function of PAPR reduction. The proposed techniques are (i) a block coding technique for PAPR reduction in O-OFDM, this approach is derived from RF-OFDM and involves block coding between the information bits and the amplitudes that have been modulated onto the subcarriers. (ii) in-band trellis coding and out-of-band carrier design is introduced to curtail the negative peaks of the electrical signal. The techniques, however, require an expanded transmission bandwidth and exhibit a substantial complexity overhead.

- *O-OFDM structure specific techniques*: In these techniques, the frame structure of O-OFDM is exploited to reduce the PAPR. (i) semi-definite relaxation based PAPR reduction method for DCOOFDM. (ii) in ellipse-based DCO-OFDM, DCO-OFDM is modified based on the concept of constant envelope OFDM to reduce PAPR.
- *Multiple signaling and probabilistic techniques*: In these techniques, numerous candidate signals containing the same information are generated and the one with lowest PAPR is selected for transmission. Most common probabilistic techniques are: (i) partial transmit sequences (PTS), (ii) selected-mapping (SLM), (iii) tone-reservation (TR) and, (iv) pilot-assisted (PA). Typically, these methods require side information to be passed on along with the data. Using side information to restore the original data block reduces the useful data rate and increases the computational complexity. [**Ali18**]

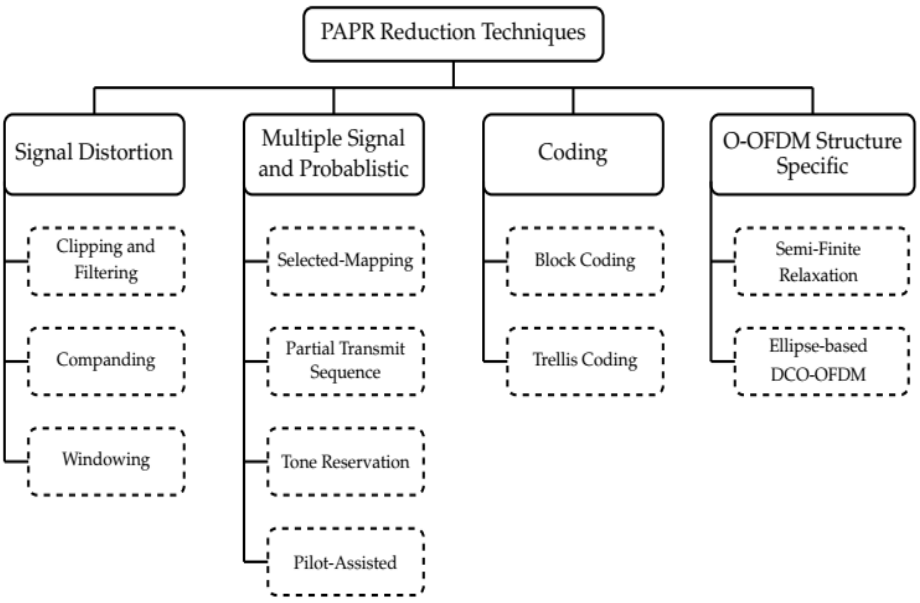

Figure 3-4: Taxonomy of PAPR reduction techniques

Among all the techniques that have been promising ones because it is simple to implement, introduces no distortion in the transmitted signal, and can achieve significant PAPR reduction is the SLM technique.

3.2.5.2. Selected-Mapping (SLM) technique:

The idea in SLM consists of converting the original data block into several independent signals, and then transmitting the signal that has the lowest PAPR. The selected signal index, called *side information index* (SI index), must also be transmitted to allow for the recovery of the data block at the receiver side, which leads to a reduction in data rate. The SI for a channel coded SLM appears explicitly in the data sequence -as a set of bits - to be encoded so that the side information is protected by the same channel code. The advantage of such an arrangement is that no additional protection is needed for side information and the rate loss due to the side information is small.

The probability of erroneous SI detection has a significant influence on the error performance of the system since the whole data block is lost every time the receiver does not detect the correct SI index.

In the SLM approach $\boldsymbol{U}$ statistically-phase sequence, say $\boldsymbol{P^{(u)} = \left[P_0^{(u)}, P_1^{(u)}, P_2^{(u)}, \ldots . P_{N-1}^{(u)}\right]^T}$ are generated where $\boldsymbol{P_K^{(u)} = exp(j\Phi_k^{(u)})}$, $\boldsymbol{\Phi_k^{(u)} \in [0, 2\pi]}$, $\boldsymbol{k = 1, 2, \ldots, N-1}$, $\boldsymbol{u = 1, 2, \ldots, U}$ then the data block $\boldsymbol{X = [X_0, X_1, X_2, \ldots, X_{N-1}]^T}$ is multiplied component-wise with each one of $\boldsymbol{U}$ different phase sequence $\boldsymbol{P^{(u)}}$, resulting in a set of $\boldsymbol{U}$ different data blocks $\boldsymbol{X^u = \left[X_0 P_0^{(u)}, X_1 P_1^{(u)}, X_2 P_2^{(u)}, \ldots . X_{N-1} P_{N-1}^{(u)}\right]^T}$. Then, all $\boldsymbol{U}$ alternative data blocks (one of the alternative subcarrier sequences must be the unchanged original one) are transformed into time domain to get transmitted symbols $\boldsymbol{x^u}$ by IFFT, where $\boldsymbol{x^u}$ are defined as the candidate signals. Finally, the one with the minimum PAPR is selected for transmitting, shown in Figure 3-5. [Paw11]

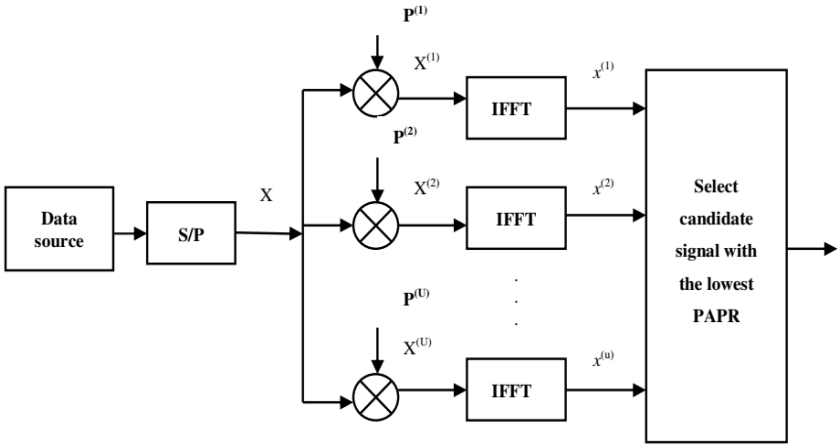

Figure 3-5: The block diagram of SLM scheme

The probability that, the PAPR of the OFDM signal exceeds a certain threshold Υ is given by

$$\boldsymbol{Pr(PAPR > \Upsilon) = 1 - (1 - exp(-\Upsilon))^N} \tag{3.5}$$

In SLM it is assumed that, $\boldsymbol{U}$ statistically independent alternative sequences, which represent the same information, are generated by some suitable means. The sequence with the lowest PAPR is selected for transmission.

The probability that, the lowest PAPR $\boldsymbol{\Upsilon_i}$ exceeds a certain threshold Υ *is* given by

$$\boldsymbol{Pr(\Upsilon_i > \Upsilon) = (Pr\{PAPR > \Upsilon\})^U} \tag{3.6}$$

where $\boldsymbol{U}$ is the number of phase sequences.

Υ is the given reference level (threshold). [Paw11]

Several improvements and variants of the SLM method have been offered to reduce its complexity besides increasing the efficiency of PAPR reduction such as Partial SLM, SLM without SI and hybrid SLM.

3.2.5.2.1. Partial SLM Method:

In this section, a method based on the SLM technique called Partial SLM. This method has better PAPR reduction performance than the conventional SLM technique with lower computational complexity. The proposed scheme works as follows: the incoming OFDM sequence $\boldsymbol{X}$ is divided into $\boldsymbol{G}$ number of sub sequences each of length Ñ. Each sub-sequence is fed into an IFFT block of length Ñ and the conventional SLM is applied in each sub-block. [**Ibr13**]

3.2.5.2.2. Selected Mapping without Side Information:

The transmitted SI bits cause bandwidth efficiency to be decreased besides, when SI is incorrectly detected by receiver, all received frames be lost. Hence, the use of channel coding is needed, which results in system complication and sacrifices data rate. channel estimation and PAPR reduction are combined in which channel estimation is performed by selecting the place of pilot tone employed inside each data block, and then power distinction between data symbols and the pilot tone is used in order to recover SI in the receiver side.

Recently, some schemes have been proposed in [**Gof08**], using permutation and m-sequence respectively to eliminate the pilot tones and displaces them with data symbols inside the data block (some transmitted symbols are extended). At the receiver side, it is tried to discover the places of the expanded symbols to recover the SI index. [**Mey12**]

3.2.5.2.3. Hybrid SLM Techniques:

In recent years, some hybrid methods have also been developed in the literature. These schemes combine two or more methods for PAPR reduction.

a. **Error Control Selected Mapping (EC-SLM):** This hybrid technique scheme proposed to enable the receiver to recover data without explicit SI bits by using Turbo coding, Turbo coding and SLM can be combined to reduce the PAPR of OFDM signal with quite moderate additional complexity. The advantage of this scheme is that the Turbo encoder is used for two purposes, error correction and PAPR reduction. This reduces the hardware complexity of the system. [**Far17**]

b. **Error Control Selected Mapping with Clipping (ECSLM-CP):** A complete hybrid scheme with one technique where modified repeats accumulate (RA) code, selected mapping, and clipping are combined. The RA code is a repetition code with an accumulator, followed by an interleaver that generates good sequences in relation to PAPR reduction and allows an improvement of BER performance. On the other hand, the EC-SLM-CP uses the modified SLM with label insertion to avoid transmitting side information, followed by a four-stage linear-feedback shift register (LFSR), and the signal is transformed into orthogonal channels by the IFFT. Finally, in the transmitter the signal is clipped in order to reduce the PAPR. This technique provides good PAPR reduction and, BER improvement, avoids transmitting side information. [**Far17**]

3.3. Simulation results and analysis:

The PAPR reduction of the SLM scheme is examined by computer simulation (Matlab). Complementary cumulative distribution function (CCDF) of PAPR of the DCO-OFDM signal obtained with the SLM technique when using 4-QAM, 16-QAM, 64-QAM, 256-QAM modulation showed the performance of SLM for different phase sequences $\boldsymbol{U}$. where, X axis of figure 3-6 to 3-9 indicates probability of PAPR represented by $PAPR_0$, the CCDF of PAPR of the original signal without SLM is also showed ($\boldsymbol{U} = 1$) in those figures. While, the applied signal frequency $f = 500$ TZh

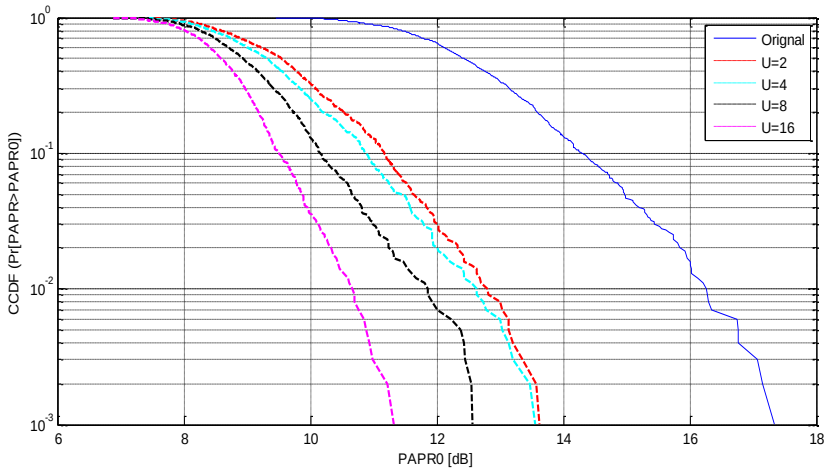

Figure 3-6: PAPR CCDF of DCO-OFDM -OFDM signal (4-QAM) with SLM reduction

Figure 3-6 shows SLM technique with $\boldsymbol{U} = 2$ improves the PAPR CCDF by 3.7 dB over the original signal. Moreover, we notice reductions in PAPR values while the numbers of phase sequences increases ($\boldsymbol{U} = 4,\ 8,\ 16$ gives $PAPR_0 = 13.6,\ 12.5,\ 11.4$ dB respectively).

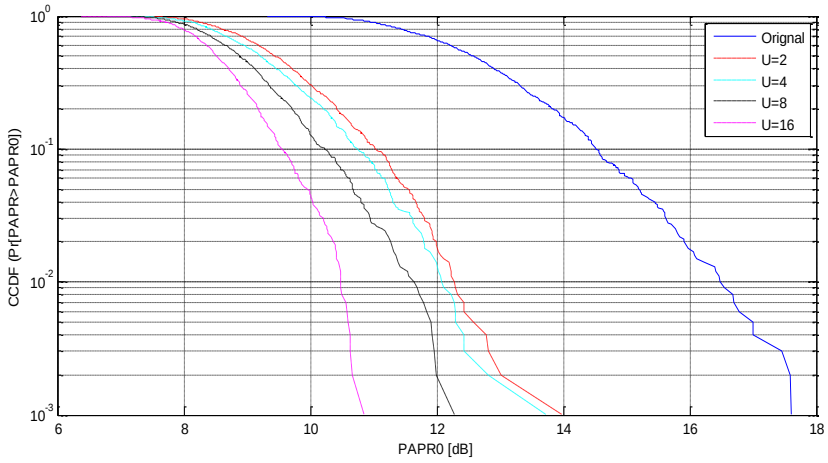

Figure 3-7: PAPR CCDF of DCO-OFDM signal (8-QAM) with SLM reduction

Figure 3-7 shows a PAPR CCDF improvement on the DCO-OFDM signal by using SLM, SLM reduces PAPR by using 16 phase sequences ($\boldsymbol{U} = 16$, $PAPR_0 = 10.9$ dB) better than

using 8, 4, or 2 phase sequences, while PAPR CCDF values in the original signal is still high even with the modulation technique has been changed to 16-QAM.

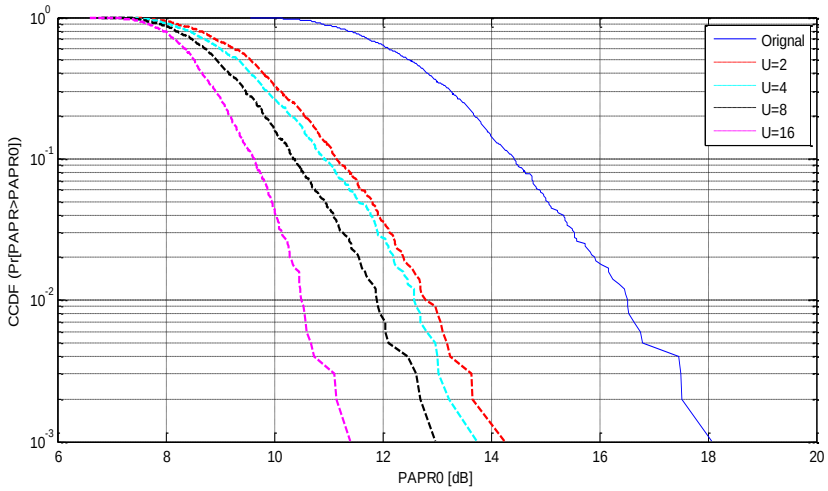

Figure 3-8: PAPR CCDF of DCO-OFDM signal (64-QAM) with SLM reduction

Figure 3-8 shows that the data modulation has been changed to 64-QAM and the original signal and the signals with SLM technique approximately have the same PAPR CCDF values in the previous experiences ($\boldsymbol{U} = 1,\ 2,\ 4,\ 8,\ 16$ gives $PAPR_0 = 18.1,\ 14.3,\ 13.7,\ 13,\ 11.4$ dB respectively).

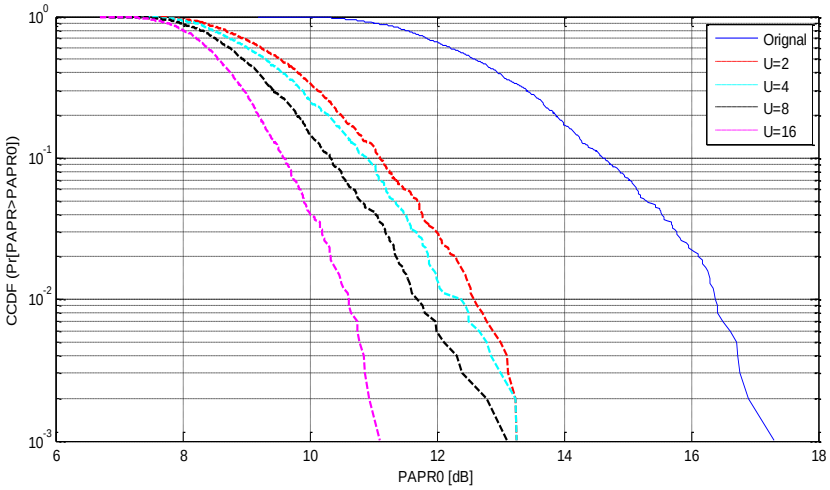

Figure 3-9: PAPR CCDF of DCO-OFDM signal (256-QAM) with SLM reduction

The results that we have in a figure 3-9 ($\boldsymbol{U} = 1,\ 2,\ 4,\ 8,\ 16$ gives $PAPR_0 = 17.4,\ 13.3,\ 13.3,\ 13.1,\ 11.1$ dB dB respectively) confirms that the SLM technique can give us great performance without needing to changing the modulation technique that mean the QAM modulation type doesn't have any influence on the performance of the SLM technique, but the number of SLM phase sequences has a huge PAPR reduction on the DCO-OFDM signals.

3.4. Conclusion:

This chapter performs a literature review on the high PAPR problem in OFDM system. It explains the occurrence of high PAPR in this system including its definition and its measurement parameters as well as the consequences of high PAPR in optical resource and the impact on SQNR in converters (ADC and DAC). It also gives an overview of different PAPR reduction techniques where we focused on SLM technique which based on dividing the data sequences into a numerous independent signals in order to transmitting the signal that has the lowest PAPR. Furthermore, we will take a look to some samples of innovative SLM are offered.

Simulation results showed SLM has a massive effect on PAPR reduction as the number of sequences increases.

FINAL CONCLUSIONS

This dissertation gives general ideas on the most useful multicarrier communication system, the Orthogonal Frequency Division Multiplexing (OFDM) designed to overcome the drawbacks of the conventional single carrier systems. The introduction of the CP in the OFDM signal solved the ISI and ICI problems caused by a dispersive channel, as long as the CP interval is higher than the delay spread. Furthermore, an equalization technique through the introduction of training symbols is used to mitigate the distortion in the OFDM symbol caused by the propagation channel. Due its several advantageous features specially the high-data rate and spectrum efficiency (using orthogonal overlapping subcarriers). OFDM has been adopted by many wireless communication standards alike LTE, WIMAX, DVB-T, ADSL, WI-FI, and VLC.

Many techniques focus on the evolution of the VLC system (concluded that an LED and a photodetector are the most commonly used sources and detectors) beside the novel approaches in the literature of the O-OFDM based system, this system by using the conventional OFDM earns a high data-rate with a robustness against a multipath channel. However, there are certain limitations we must deal with alike the O-OFDM signal must be real and non-negative, the mandatory of LoS condition and Limited transmission range, for that reason many OFDM forms designed in order to fit the LEDs functions requirements such as DCO-OFDM and ACO-OFDM.

Despite numerous beneficiary features of O-OFDM system, synchronization and high PAPR are major issues of this system. So, for the complete exploitation these tremendous features of O-OFDM system, these two major problems should be resolved. This dissertation concerned to reduce the inherent problem of high PAPR in O-OFDM system by presenting a literature review on PAPR, impact of PAPR on the performance and different established methods to reduce the PAPR.

The main reason of occurrence of high PAPR in O-OFDM is due the addition data symbols across a number of independent modulated subcarriers, the impact of large peaks is increasing the level of distortion and the SQNR (Signal-to-Quantization Noise Ratio) present in the transmitted signal. One of the promising PAPR reductions is the SLM technique because it is simple to implement (converting the same data block into several independent sequences to transmit the lowest PAPR), introduces no distortion in the transmitted signal, and can achieve significant PAPR.

In other hand, the simulation results showed that we can depend on SLM technique to apply a PAPR reduction with high performance.

References

[**Ain14**] Anil Khatiwada" A Thesis report on PAPR reduction in OFDM System Using Partial Transmit Sequence (PTS) and Precoding Techniques" Thapar University, India, 2014.

[**Ali18**] Ali Waqar Azim "Signal Processing Techniques for Optical Wireless Communication Systems. (Optics /Photonic)" Grenoble Alpes University, 2018.

[**Ake88**] D. Akerberg "Properties of a TDMA pico cellular office communication system" IEEE Global Telecommunications Conference and Exhibition. Communications for the Information Age Dec. 1988.

[**Dad75**] C.E. Dadson, J. Durkin and R.E. Martin "Computer prediction of field strength in the planning of radio systems" IEEE Transactions on Vehicular Technology, February 1975.

[**Fab10**] / Fabiana Ferraro "A thesis report on Study And Analysis Of An Optical OFDM Based On The Discrete Hartley Transform For IM/DD Systems" polytechnic University of Cataloni, 2010.

[**Far17**] Francisco Sandoval, and Gwenael Poitau, and Francois Gagnon "Hybrid Peak-to-Average Power Ratio Reduction Techniques: Review and Performance Comparison" Article in IEEE Access, Article page(s): 27145 – 27161,November 2017.

[**Gof08**] S. Y. L. Goff, B. K. Khoo, C. C. Tsimenidis, B. S. Sharif "A Novel Selected Mapping Technique for PAPR Reduction in OFDM Systems", IEEE Transactions on Communication, Article page(s): 1775 – 1779, November, 2008.

[**Ibn04**] Mohamed Ibnkahla "Signal Processing for Mobile Communications Handbook" Ph.D, National Polytechnic Institute of Toulouse, 2004.

[**Ibr13**] Ibrahim Mohammad Hussain "Low Complexity Partial SLM Technique for PAPR Reduction in OFDM Transmitters "Sir Syed University of Engineering and Technology, Karachi, Pakistan march 2013.

[**Jos12**] H. D. Joshi "Performance augmentation of OFDM system," Ph.D. dissertation, Jaypee University of engineering and Technology, India, May 2012.

[**Key20**]http://rfmw.em.keysight.com/wireless/helpfiles/89600b/webhelp/subsystems/wlan-ofdm /Content/ofdm_ basicprinciplesoverview. htm, 01/06/2020

[**Lon68**] Longley A.G and Rice P.I "Prediction of tropospheric radio transmission loss over irregular terrain A computer method-1968;

[**Mey12**] S. Meymanatabadi , M. J. Musevi Niya, B. Mozaffari Tazehkand "An Efficient Scheme for PAPR Reduction of OFDM Based on Selected Mapping Without Side Information" 2012.

[**Paw11**] Pawan Sharma and Seema Verma "PAPR reduction of OFDM signals using Selective Mapping with Turbo codes" International Journal of Computer Applications, August 2011.

[**Ped18**] Pedro Lourenço Farias Carrilho de Oliveira "A Thesis report on Study and Implementation of a VLC-OFDM System/, University of Lisbon 2018.

[**Rap96**] Rappaport.T.S " Wireless Communications: Principles and Practice" *Prentice Hall, New York*, 1996

[**Sei92**] S.Y. Seidel and T.S. Rappaport "914 MHz path loss prediction models for indoor wireless communications in multifloored buildings" IEEE Transactions on Antennas and Propagation Feb 1992.

[**Wik20**] wikipedia.org.

[**Yon10**] Yong Soo Cho "MIMO-OFDM wireless communications with MATLAB" Chung-Ang University, Republic of Korea, 2010.